TRACK TRAIN DYNAMICS TECHNICAL DOCUMENTATION

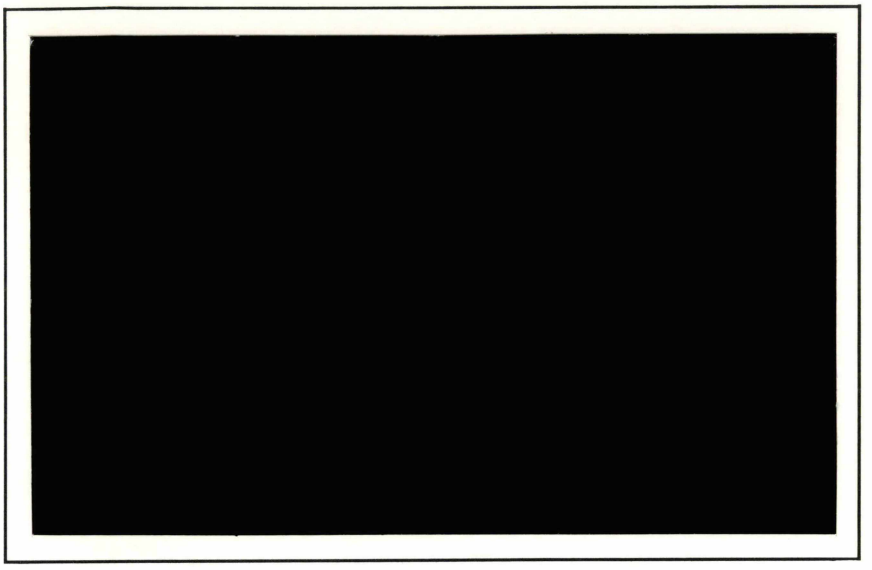

AAR

An International Government-Industry
esearch Program on Track-Train Dynamics

HIGH PERFORMANCE, HIGH CUBE
COVERED HOPPER PROGRAM
BASE CAR DYNAMIC PERFORMANCE TESTS
VOLUME 4 - SUMMARY

REPORT NO. R-581

S.F. Kalaycioglu

S.K. Punwani

June, 1984

AAR Technical Center

Chicago, Illinois

1. REPORT NO.	2. REPORT DATE	3. PERIOD COVERED
R-581	June, 1984	Dec. 1983 thru May, 1984

4. TITLE AND SUBTITLE
High Performance, High Cube Covered Hopper Program, Base Car Dynamic Performance Tests, Volume 4 - Summary

5. AUTHOR(S)
Semih F. Kalaycioglu, Sr. Engineer/Analyst and Swamidas K. Punwani, Asst. Mgr., Applied Technology

6. PERFORMING ORGANIZATION NAME AND ADDRESS
Association of American Railroads
Track Train Dynamics
3140 S. Federal Street
Chicago, Illinois 60616

7. TYPE OF REPORT
Research

8. CONTRACT OR GRANT NO.
DTFR-53-82-C-00251

9. SPONSORING AGENCY NAME AND ADDRESS
Federal Railroad Administration
400 7th Street, S.W.
Washington, DC 20590

10. NO. OF PAGES
59

11. NO. OF REFERENCES
6

12. SUPPLEMENTARY NOTES Part of the Track Train Dynamics High Cube, High Performance Covered Hopper Program

13. ABSTRACT

This report presents a summary of the dynamic performance tests of a 4750 cubic foot capacity high cube covered hopper car. All the tests were conducted at the Transportation Test Center in Pueblo, Colorado. Results of the reduction and analysis of test data for the rock-and-roll, pitch-and-bounce, hunting, curving and bunched spiral regimes are briefly presented. These results establish the overall performance of the base car, in accordance with the performance guideline format, and will be used as the standard with which new prototype car designs will be compared. The test program is part of the Track Train Dynamics High Cube, High Performance Covered Hopper Car Project.

14. SUBJECT TERMS Angle-of-attack; Covered Hopper Car Tests; Curving; Hunting; Pitch-and-bounce; Rock-and-roll; Roll Angles: Spiral Twist; Vertical and Lateral Accelerations; Wear Index

15. AVAILABILITY STATEMENT
Assistant Vice President
AAR Technical Center
3140 S. Federal Street
Chicago, Illinois 60616

EXECUTIVE SUMMARY

The High Performance, High Cube Covered Hopper Car Project was initiated in June, 1980, as part of the Track Train Dynamics Program (TTD), with a view to promoting improved car designs. The supply industry was invited to develop and submit improved prototype cars for testing. Performance guidelines were issued for new design cars and a test program was outlined. The project stipulated that all cars of improved design would be compared against a "base" car of current design. A test base car was obtained on loan from the Missouri Pacific Railroad and performance tests were conducted on various test tracks at the Transportation Test Center in Pueblo, Colorado.

The detailed results of the base car tests were reported in previous TTD publications. This document serves as a summary report for the performance of the vehicle in the rock-and-roll, bounce, hunting and curving regimes.

For rock-and-roll, the performance of the vehicle was described in terms of the car body roll angles and vertical wheel loads, particularly with respect to wheel lift and suspension system spring travel. The empty car experienced its critical rock-and-roll speed near 24/25 mph, with a peak-to-peak car body roll angle of 9.3 degrees and associated wheel lifts of short duration. The loaded car, however, experienced its critical speed near 16/17 mph, and the corresponding peak-to-peak roll angle was as high as 10.6 degrees. Extended wheel unloadings over track lengths of 6 feet were observed at test speeds of

15 to 19 mph. For both tangent and curved track, the roll responses of the vehicle in both the empty and loaded conditions were comparable.

For the bounce regime, the vertical accelerations at the car body center plate and vertical wheel loads were characterized. The critical bounce and pitch speeds of the vehicle were determined to be 56 mph. Peak vertical accelerations of up to 1.2 g, and dynamic load factors of 1.8, associated with solid spring bottomings, were noted at the bounce resonance speed.

The hunting tests utilized three different wheel profiles: the CN Heumann (Radford), Ø.3 conicity and AAR 1:2Ø. Lateral car body and truck accelerations were used to characterize the hunting performance.

The "onset" hunting speed for all three wheel profile configurations was defined. The CN Heumann (Radford) profile was associated with a hunting onset speed of 51 mph, as opposed to 45 mph for the Ø.3 conicity wheel. The data indicated that a root-mean-square (rms) acceleration level of Ø.1 g was the threshold that could be used to identify the onset hunting speed. It was also found that the vehicle first experienced instability at the leading end, which involved coupled motions of both the car body and truck. The AAR 1:2Ø wheel profile provided lateral stability up to 75 mph. However, at 82 mph the onset of hunting in both the leading and trailing end car body and trucks was noted. At the leading end, fully sustained hunting oscillations, accompanied by hard flanging, occurred at speeds above 55 mph for both the CN Heumann (Radford) and Ø.3 conicity

wheel profiles, with rms accelerations exceeding the Ø.3 g level.

The curving tests were conducted on test tracks that provided curvatures ranging from 5Ø minutes to 7-1/2 degrees. Mean values of lateral and vertical wheel loads, L/V ratios and angles-of-attack were used to characterize the curving performance of the base car.

In general, the lateral load increased with track curvature, with the high rail loads increasing and the low rail loads decreasing with increasing speeds. The peak L/V ratios, continuously sustained over 6 feet of track, were found to approach the critical level for wheel climb, as described in the performance guidelines. The corresponding maximum lateral loads were also about 8Ø% of the critical levels.

The angle-of-attack data conformed to expectations, in which the leading wheelset had higher angles-of-attack, which increased with track curvature and indicated that the leading wheelset during curve negotiation trailed the radial line extending from the center of the curve through the center of the wheelset axle. The trailing wheelset, however, held to a near radial position with minimal angles-of-attack.

Extended vertical wheel unloadings, of up to 1ØØ milliseconds duration, were seen on the inner wheel of the leading wheelset on a bunched spiral, where a 4-1/2 inch superelevation was attained over a 12Ø-foot segment of the 3ØØ-foot spiral.

ACKNOWLEDGMENTS

The authors sincerely acknowledge their indebtedness to the Federal Railroad Administration for funding the Covered Hopper Car Test Program and for providing invaluable technical support during all phases of the test program. Special appreciation is expressed to Ms. Claire Orth and Mr. Alfred G. Bowers of the Federal Railroad Administration for their technical inputs.

The authors also wish to acknowledge Mr. Keith L. Hawthorne, AAR Technical Director, and Mr. Roy A. Allen, Manager - Applied Technology, for their helpful guidance and encouragement throughout the test program.

The authors extend their appreciation to Mr. Niranjan Haralalka for his assistance in the data reduction and preparation of this report.

Special thanks to the crew members of the AAR-100 Research Car, Messrs. Frank Hirsch, Bill Sneed, Ron Bidwell, Jim Rzonca, Don Waldo and Alex Harell.

Thanks are also expressed to Messrs. Osman Ahmad, Sean Judd and Bill Drish for their help in the test data reduction.

The authors thank the Missouri Pacific Railroad for the loan of the base covered hopper car to the Track Train Dynamics program for use in the test program.

The authors also wish to express their appreciation to Dr. Robert Breese for his editorial assistance and direction in the preparation of this report.

LIST OF SYMBOLS AND ABBREVIATIONS

Symbol (or) Abbreviation	Definition
AR4	A-end (leading), right side, fourth axle of the vehicle.
AL4	A-end (leading), left side, fourth axle of the vehicle.
L/V	Ratio of lateral to vertical wheel load.
LIM	Linear Induction Motor (the name of the track where the rock-and-roll tests were conducted).
RTT	Railroad Test Track (the name of the track where the hunting tests were conducted).
TDT	Train Dynamics Track (the name of the track where the one and one-half degree curving tests were conducted).
FAST	Facility For Accelerated Service Testing (the name of the track where the three-, four- and five-degree curving tests were conducted).
BALLOON LOOP	Balloon Loop (the name of the turn-around track where the curved track, rock-and-roll and seven and one-half degree curving tests were conducted).
CG	Center of gravity.
L5	The level that is exceeded ninety-five percent of the time.
L95	The level that is exceeded five percent of the time.
LTD6MIN	The minimum of all levels that are continuously sustained over a six-foot lentgh of track.
LTD6MAX	The maximum of of all levels that are continuously sustained over a six-foot lentgh of track.
RMS	Root mean square
STD	Standard deviation

TABLE OF CONTENTS

LIST OF TABLES

LIST OF FIGURES

LIST OF FIGURES (Continued)

LIST OF FIGURES (Continued)

1.Ø INTRODUCTION

The detailed results of the base car tests have been reported in previous TTD publications [2,3,4].* This document serves as a summary report for the performance of the vehicle in the rock-and-roll, pitch-and-bounce, hunting and curving regimes.

2.Ø TEST PROGRAM

In June, 198Ø, The Track Train Dynamics Program published Performance Guidelines [1] for high performance, high cube covered hopper cars to encourage the development of improved covered hopper cars. The guidelines described the minimum requirements for the dynamic performance of the prototype vehicles in the rock-and-roll, pitch-and-bounce, hunting and curving regimes. The project plan called for the testing of a current design (base line case) of covered hopper car, with which each new prototype car would be compared. The base car, obtained on loan from the Missouri Pacific Railroad for use in the test program, was a 1ØØ-ton covered hopper car, with a cubic capacity of 475Ø feet and a truck-center distance of 45 feet, 9 inches. The car was equipped with conventional three-piece trucks, with constant-column friction damping truck suspension systems and conventional double-roller side bearings.

---

*Numbers in square brackets [] indicate the references listed in Section 7.Ø of this report.

2.1 Test Regimes

The test program was designed around available track sites at the Transportation Test Center (TTC) in Pueblo, Colorado. The test consist included, in order, a four-axle locomotive, the AAR-100 Research Car, a loaded 100-ton open top hopper car, serving as a buffer car, the test car, and a follow-on buffer car. A brief description of the test program in each performance regime is given in the following sections.

The rock-and-roll runs were conducted in four separate test series: tangent and curved track, test car empty and loaded. The tangent track tests were run on the LIM (linear induction motor) track, over a 400-foot perturbed track section with a 0.75-inch cross elevation difference. The curved track rock-and-roll series were run on a 400-foot (10 rail length) perturbed track section, which was part of the Balloon loop. Speeds for each series were selected in order to identify the peak response to within 1 mph of the true resonance condition. The bounce runs, both empty and loaded, were run over a perturbed track section on the LIM track. Parallel (non-staggered) track surface profiles with a 0.75-inch maximum amplitude deviation were used.

Curving tests were run for both the empty and loaded car, although the principal effort was directed at the loaded car case. The curves that were available as test zones were 50 minutes (RTT); 1.5 degrees (TDT); 3.0, 4.0 and 5.0 degrees (FAST); and 7.5 degrees (Balloon). Test runs were made in both the clockwise (CW) and counterclockwise (CCW) directions at five different speeds, including underbalance, balance, and overbalance

conditions. The single exception was the 50-minute curve where the balance speed was 105 mph and thus only underbalance test runs could be conducted. Curve entry and curve spirals were also part of the data collection. The existing spiral into the 7-1/2 degree curved track was modified to configure it for severe track twist; the superelevation was made to increase from zero to 4-1/2 inches over a 120-foot length of track.

The hunting series were run on the RTT track with the empty car only, but including three separate series, using the following wheel profiles: CN Heumann (Radford), new standard AAR 1:20 and a 0.3 conicity, (see Appendix A), which was broadly representative of a worn wheel profile. Test runs, for each hunting series, started at a nominal speed of 35 mph, increasing in 5 mph increments until a flange-to-flange hunting condition was observed, or the 80 mph speed limit was reached. Additional runs were made at intermediate speeds to identify the "onset" of truck hunting.

2.2 Instrumentation and Data Collection

The AAR-100 Research Car was upgraded for the data acquisition; a PDP 11/34 computer, an ANDS-5400 analog-to-digital converter and other peripheral equipment were installed on this car. The system was run under control of GPAQ, a general purpose data collection software program, which was updated to function around the AAR-100 hardware. In all cases, a sampling rate of 256 samples per second per channel was used during the data collection.

Data were collected in each test regime, using various transducers that would best characterize the dynamic

performance of the vehicle in that particular test regime. These included lateral and vertical accelerometers, displacement transducers, roll gyros, angle-of-attack probes and two instrumented wheelsets. A detailed description of the instrumentation can be found in [2,3,4]. The instrumented wheelsets were of the IIT Research Institute design, which utilized a real-time microprocessor for each wheelset, providing continuous lateral and vertical wheel loads and L/V ratios [5].

2.3 Data Reduction and Analysis

The digital data were first converted to DECSYSTEM-2060 Computer format and the resulting voltage time histories subsequently converted to engineering units, using the calibration signals collected prior to the start of data collection. The reduction and analysis were accomplished by utilizing modern statistical and spectral techniques for physical data analysis [6]. The key parameters selected to quantify the performance of the vehicle and their analytical tools are described in the following sections.

3.0 PERTURBED TRACK TESTS

3.1 Rock-and-roll Regime

The primary objectives of the data reduction and analysis in the rock-and-roll regime were to determine the effects of extreme car body roll on the low speed operation of the base covered hopper car, while running over a perturbed track with staggered rail joints. The key parameters used to describe the

performance of the vehicle were:

1) Peak-to-peak car body roll angle.

This parameter was used to identify the critical rock-and-roll speed of the vehicle.

2) Vertical wheel loads.

Maximum and minimum levels of the vertical wheel loads, together with their associated time durations, were obtained at the leading wheelset of the leading truck, and the dynamic wheel loading and unloading were investigated. The statistical descriptors used to quantify the maximum levels of the wheel loads were the peak and L95 values. The L95 value of a parameter was defined as a level which was exceeded only 5 percent of the total time. The wheel unloading was described in terms of a minimum "peak" load and a minimum load level, called LTD6MIN, that was sustained continuously over a 6-foot track segment [2,3,4].

As noted previously, the tangent and curved track rock-and-roll series were run on a 400-foot (10 rail length) perturbed track section with a 0.75-inch cross elevation difference.

3.1.1 Tangent Track Rock-and-roll

The harmonic roll performance of the vehicle was evaluated in both the empty and loaded conditions. The resonance condition of the empty car, occurring at a speed where the car body experienced its maximum roll angle, was determined to be at 24.84 mph. In

Figure 1, the maximum peak-to-peak roll angles are plotted as a function of speed, and in which the maximum roll angles are 9.3 degrees at the trailing end and 8.9 degrees at the leading end of the vehicle. Results of the analysis of the vertical loads, shown in Figure 2, indicate that both the left and right wheels of the leading wheelset experienced wheel lifts, with short time durations, in every cycle of their motion. However, the minimum wheel loads that were continuously sustained over 6 feet of track were on the order of 2,000 lbs, which represented a 70% wheel unloading.

To illustrate the peak response of the loaded car and to show the location of its critical speed, the maximum peak-to-peak roll angles were plotted against speed, as shown in Figure 3. The peak response of the vehicle occurred near 17 mph, with a maximum peak-to-peak roll angle of 10.6 degrees.

The maximum and minimum levels of the vertical wheel loads are shown in Figure 4. The peak vertical loads of up to 78,000 lbs that were experienced near the critical roll speed of the vehicle represented a dynamic load factor of 2.4. At test speeds of 15.5 to 18.5 mph, extreme wheel unloadings were noted; the LTD6MIN levels of the vertical wheel loads were as low as 2,000 lbs, indicating a 93% wheel unloading for 250 milliseconds. Throughout the same speed range, it was noted that the suspension springs experienced solid bottoming, and corresponding peak-to-peak spring travels of up to 3.0 inches were noted.

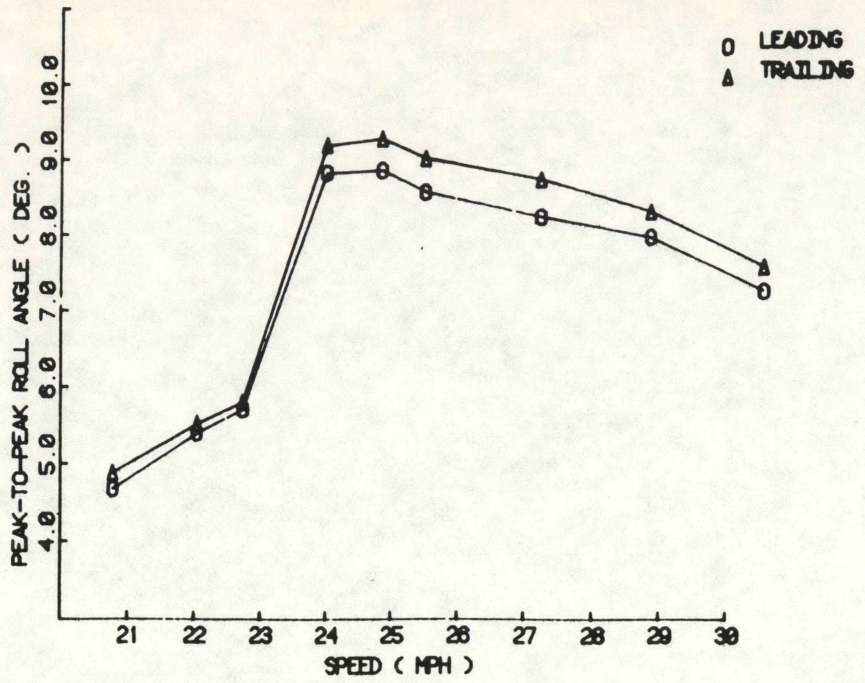

Figure 1. Car Body Roll Angle vs. Speed, for the Empty Car in the Rock-and-roll Regime on Tangent Track.

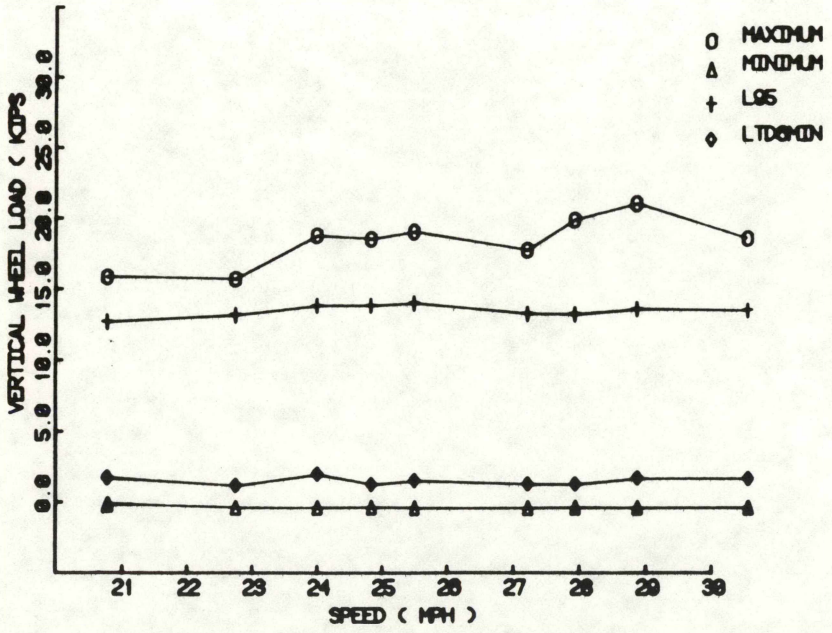

Figure 2. Vertical Wheel Load vs. Speed, for the Empty Car in the Rock-and-roll Regime on Tangent Track.

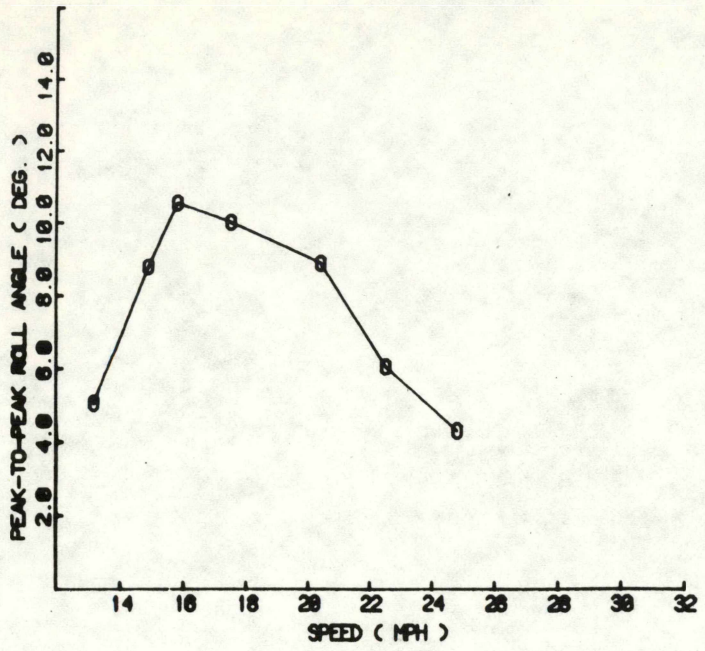

Figure 3. Car Body Roll Angle vs. Speed, for the Loaded Car in the Rock-and-roll Regime on Tangent Track.

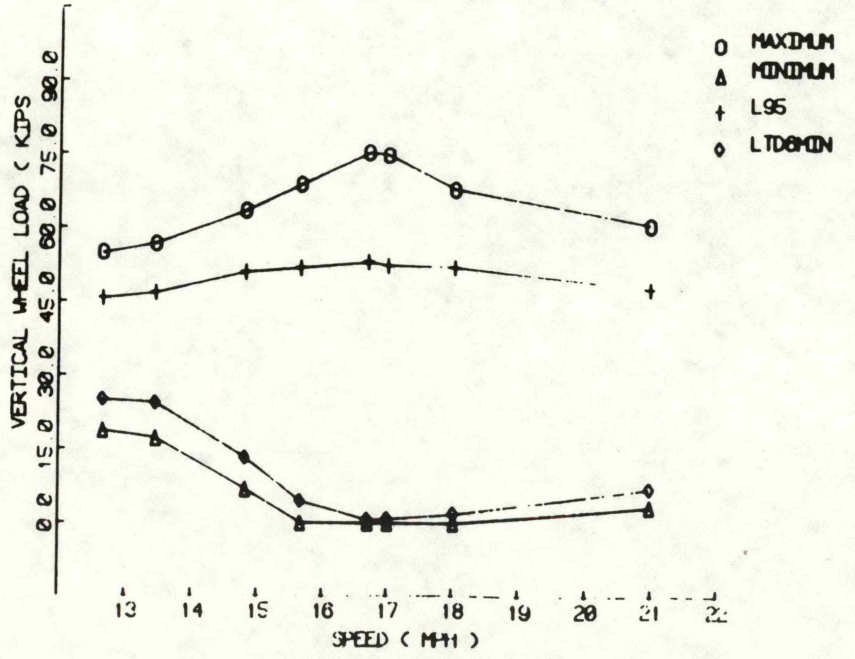

Figure 4. Vertical Wheel Load vs. Speed, for the Loaded Car in the Rock-and-roll Regime on Tangent Track.

3.1.2 Curved Track Rock-and-roll

The data from the curved track rock-and-roll tests were analyzed to determine the effects of high degrees of curvature on the harmonic roll of the vehicle. In the empty car configuration, the results of the analysis indicated that the vehicle experienced its maximum response at 24.3 mph. The corresponding maximum peak-to-peak roll angle was 9.3 degrees on the trailing end, as shown in Figure 5. Wheel lifts occurred in each cycle of the motion, along with maximum loads that exceeded twice the static load levels, as shown in Figure 6.

In the case of the loaded car, the maximum response of the vehicle was attained near 18 mph. Figure 7 shows the maximum peak-to-peak roll angles as a function of speed; the peak maximum roll angle was about 9.8 degrees.

The vertical wheel loads produced during harmonic roll of the vehicle showed a consistent trend, in which the low rail loads were higher than the high rail loads at most of the test speeds. At speeds of 15.5 to 18.5 mph, however, extended wheel lifts were experienced on the high rail, as indicated by the zero values of LTD6MIN in Figure 8. The corresponding maximum peak load of 68,500 lbs indicated a dynamic load factor of 2.1. On the low-rail side, a wheel lift with relatively short duration was noted only near the critical speed, and the LTD6MAX loads were much higher, demonstrating less sustained wheel unloading.

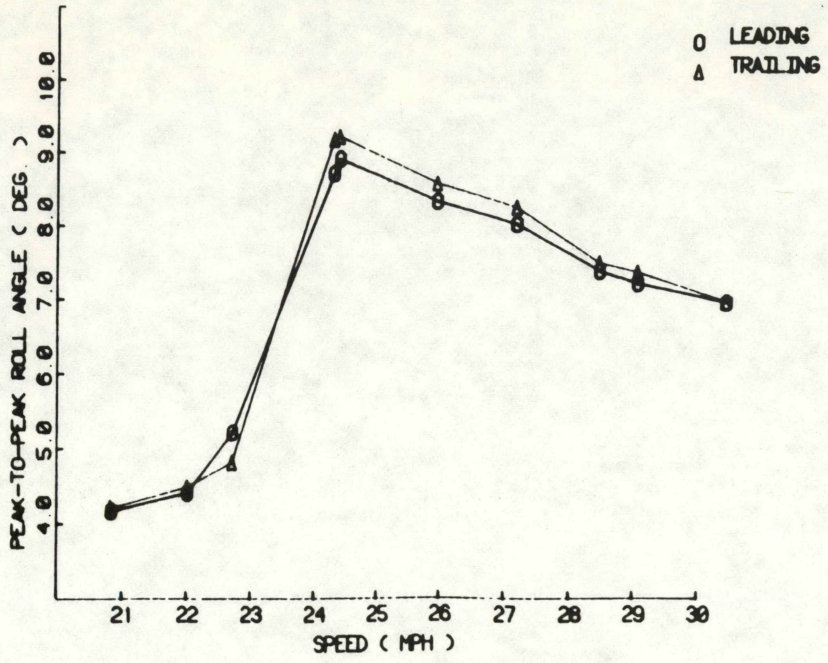

Figure 5. Car Body Roll Angle vs. Speed, for the Empty Car in the Rock-and-roll Regime on Curved Track.

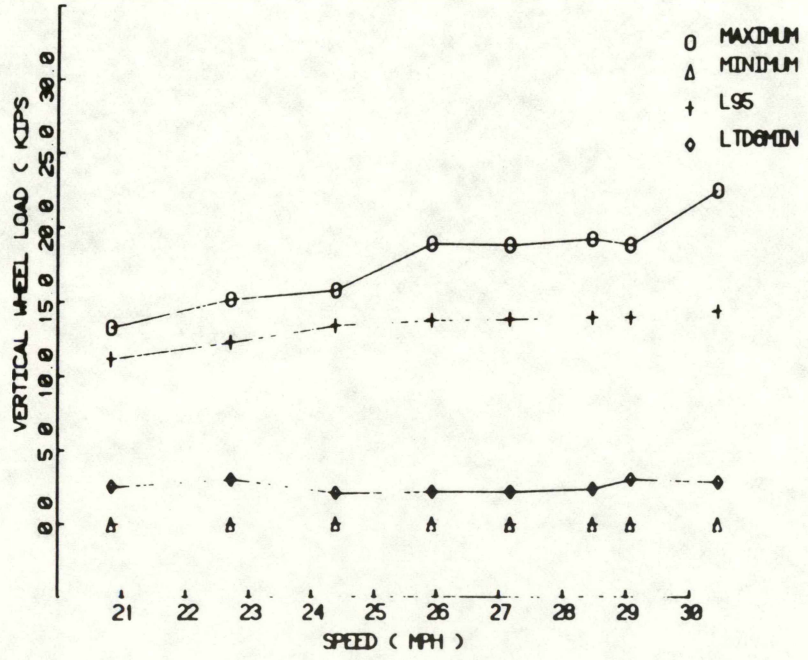

Figure 6. Vertical Wheel Load vs. Speed, for the Empty Car in the Rock-and-roll Regime on Curved Track.

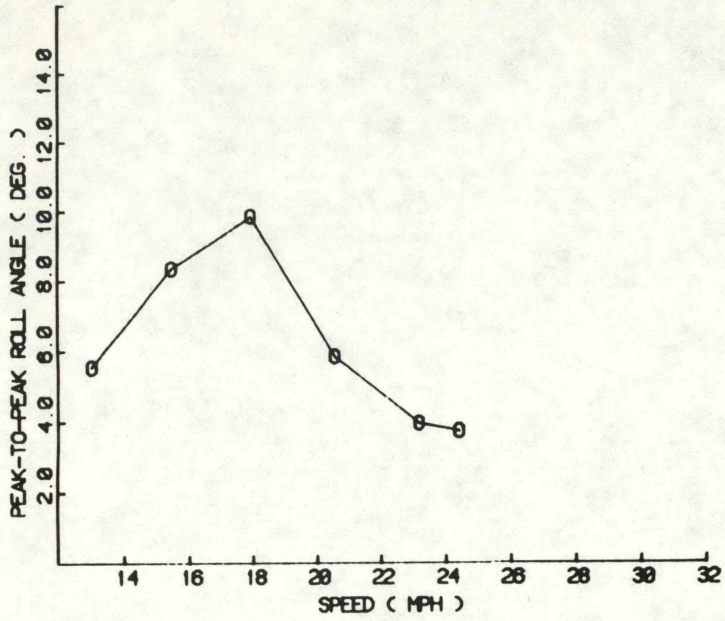

Figure 7. Car Body Roll Angle vs. Speed, for the Loaded Car in the Rock-and-roll Regime on Curved Track.

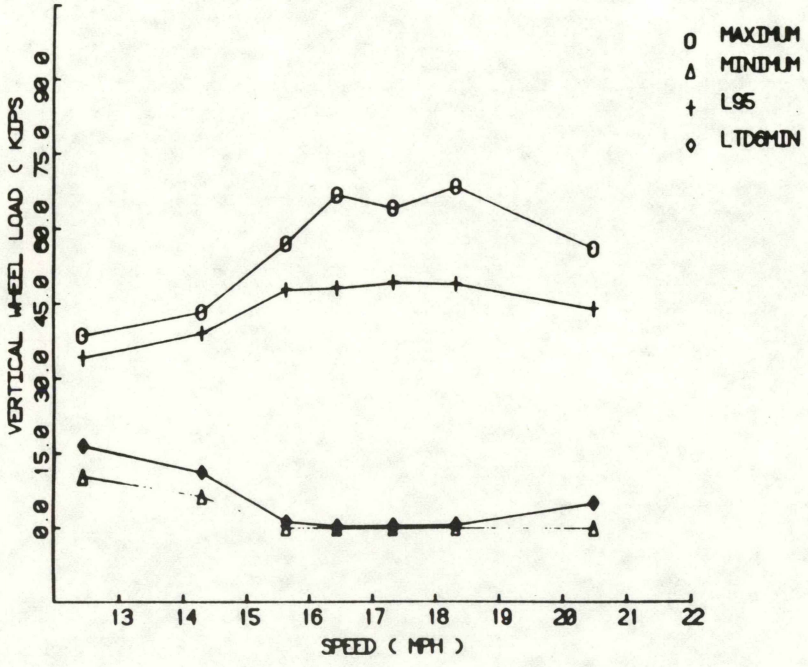

Figure 8. Vertical Wheel Load vs. Speed, for the Loaded Car in the Rock-and-roll Regime on Curved Track.

3.1.3 Comparison of Roll Response on Tangent and Curved Track

From the results presented above, the following comparisons regarding the roll response of the vehicle on tangent and curved track could be made:

a. The track curvature did not affect the resonant roll speed of the empty car; the maximum roll response of the vehicle was attained near 24/25 mph for both the tangent and curved test runs. For most of the test speeds, the empty car body rolled more on tangent track than on curved track, but in both cases maximum peak-to-peak roll angles of 9.3 degrees were measured on the trailing end of the vehicle. In both cases, the roll motion amplitudes were slightly higher for the trailing end of the car body, which may have resulted, in part, from the coupled roll and yaw motions of the car body, and partly from the asymmetric suspension characteristics of the leading and trailing trucks. Another observation worth mentioning is that the amplitudes of the harmonic roll motions of the empty car rapidly increased to a peak value and remained at high levels above the critical speed, indicating a lack of effective damping in the empty car condition. This was attributed to the insufficient motion between the truck bolster and side frames, caused by the locking action of the friction wedges when they do not slide.

b. Results of the vertical wheel loads measured on the

leading wheelset of the empty car were comparable for both tangent and curved tracks. Dynamic wheel load factors exceeding twice the static loads and wheel lifts of short duration were noted in all test runs. It was evident that the peak loads were not developed at the same speeds as those for the maximum roll angles, however, the sharp peaks in each cycle of the motion were spaced 39 feet apart, corresponding to the locations of the rail joints.

c. In the case of the loaded car, the resonant roll speeds for the tangent and curved tracks did not coincide, but were close. However, there was no measurement made at 17 mph (the critical speed on tangent track) on the curved track, and the trend of the roll amplitude curve showed that a peak response might have existed near 17 mph. Hence, a general conclusion regarding the roll response of the vehicle is that the critical speed of the vehicle was not affected by track curvature, and it occurred when the car body roll natural frequency, Ø.65 Hertz, coincided with the rail joint input frequency. Unlike the empty car, the amplitudes of the roll oscillations of the loaded car rapidly decreased at speeds beyond the critical speed of the vehicle, indicating a high damping capacity of the vehicle suspension system. As noted for the empty car condition, the loaded car body rolled more on tangent track than curved track, for most test speeds.

d. Results of the analysis of the vertical loads on the loaded car indicated that, unlike the empty car, the peak maximum wheel loads were developed at speeds near the resonant roll speed of the loaded car. The dynamic wheel loads measured on tangent track were higher than those on curved track. This may have been due in part to the fact that the tangent (LIM) track had a stiffer ballast than the curved (Balloon) track. The existing AAR specification, regarding the rock-and-roll performance of freight cars, recommends a maximum peak-to-peak roll angle of 6 degrees and a maximum of 75% wheel unloading. The results presented above indicate that the base car failed to fulfill these rock-and-roll performance requirements.

3.2 Pitch-and-bounce Regime

The observations made during the empty car bounce tests indicated that there was no evidence of a clear resonant response of the vehicle at speeds up to 70 mph. Therefore, only the results for the loaded car in the bounce regime were reported.

In order to evaluate the dynamic performance of the vehicle in the bounce regime, parameters which described the car body motion in the vertical plane were selected. Vertical acceleration measurements made near the center plate locations at the leading and trailing ends of the car body were used to identify the critical bounce speed of the vehicle. The acceleration response of the car body was evaluated in the frequency range of 0 to 20

Hertz, by low-pass filtering the acceleration time histories at 20 Hertz. The leading wheelset vertical wheel loads were investigated to quantify the dynamic effects of unstaggered tangent track perturbations. The bounce runs were conducted on the LIM track over a 400-foot section of non-staggered track with, maximum perturbation amplitudes of 0.75 inch.

Analysis of the vertical car body accelerations indicated that the loaded car body vibrated at its input excitation frequencies and higher harmonics. At speeds of 20 to 45 mph, the vertical vibrations of the car body displayed lower amplitudes. The vibrations were accentuated when the frequency with which the car passed the 39-foot rail joints approached the natural frequency of the car body on its suspension system. The critical bounce speed of the vehicle was determined to be 56.3 mph, which also coincided with the critical pitch speed. The frequency of the motions associated with the bounce and pitch motions were 2.1 and 3.0 Hertz, respectively.

The accelerations recorded on the rear end of the vehicle were higher than those on the front end, which indicated a pitch motion. Maximum peaks of 0.9 and 1.2 g were noted at 56.3 mph, for the leading and trailing ends, respectively. The maximum rms bounce acceleration of the car body, Figure 9, was approximately 0.39 g and the corresponding pitch acceleration was 0.24 radians per second per second, Figure 10..

The wheel load time histories showed that a steady-state-like response was achieved after a few seconds into the perturbed track section. The dynamic vertical load factors developed during the

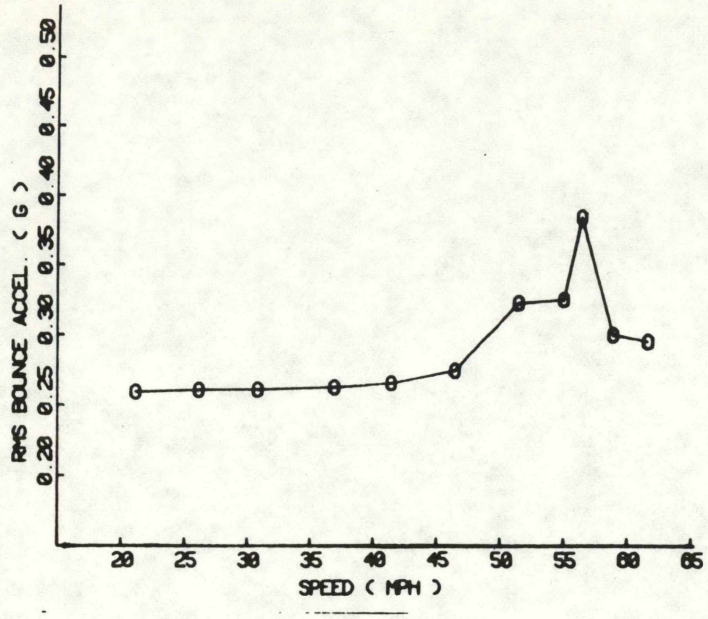

Figure 9. Root-mean-square Bounce Acceleration vs. Speed, for the Loaded Car in the Pitch-and-bounce Regime on Tangent Track.

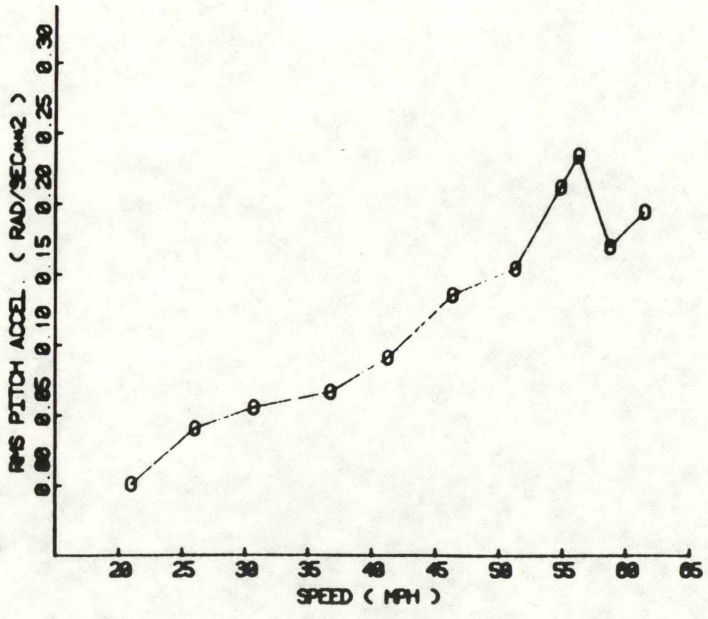

Figure 10. Root-mean-square Pitch Acceleration vs. Speed, for the Loaded Car in the Pitch-and-bounce Regime on Tangent Track.

extreme pitch and bounce motions of the vehicle were on the order of 1.8. Wheel lifts did not occur at any test speed. A maximum of 60% wheel unloading, sustained over 20 milliseconds, was noted at the resonant speed of the vehicle.

It was observed that the vehicle, undergoing pitch and bounce motions on the perturbed track, developed its highest amplitude response at its corresponding critical speed. Figure 11 shows the leading axle right wheel vertical load as a function of speed, where maximum loads of up to 58,000 lbs and minimum loads of 9,500 lbs were noted at 56.3 mph. Spring bottoming, with a total spring travel of approximately 3.0 inches, was also measured at this speed, as shown in Figure 12.

4.0 HUNTING REGIME

The test data for the hunting regime were reduced and analyzed in accordance with the requirements of the dynamic performance of the vehicle, as indicated in the performance guidelines. The field test data regarding the lateral stability of the vehicle were found to be reliable and fairly consistent, and the results were in close agreement with the findings of similar test programs.

The performance of the vehicle was characterized by using the lateral accelerations measured on the car body and trucks, and the wheel/rail displacements and forces in the test configuration which utilized the CN Heumann (Radford) wheel profile.

The lateral accelerations measured at the car body center of gravity on the leading and trailing ends, and on the leading axles

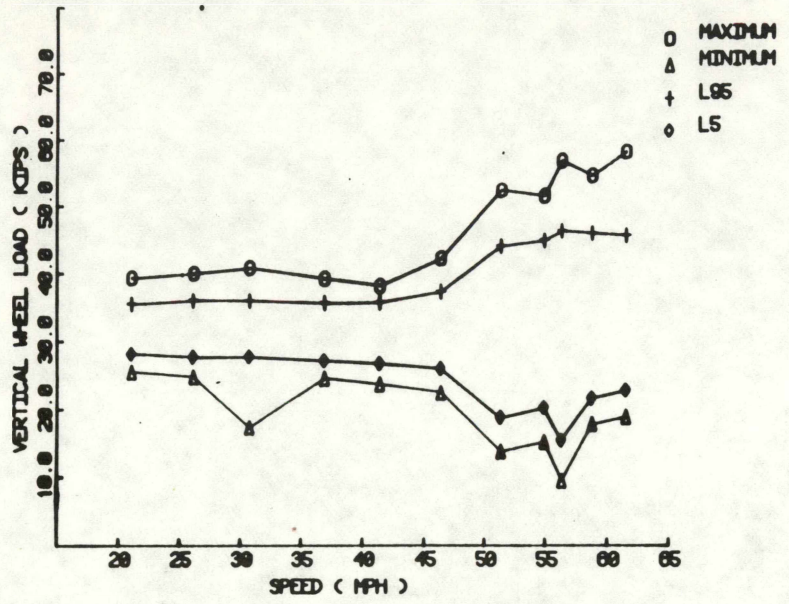

Figure 11. Vertical Wheel Load vs. Speed, for the Loaded Car in the Pitch-and-bounce Regime on Tangent Track.

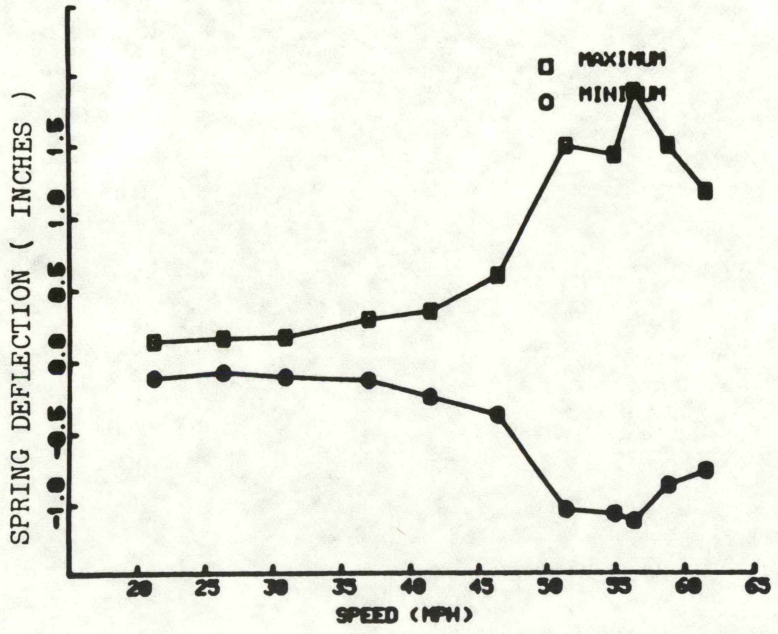

Figure 12. Spring Deflection vs. Speed, for the Loaded Car in the Pitch-and-bounce Regime on Tangent Track.

of the leading and trailing trucks were used to identify the "onset speed" of hunting.

The critical hunting speed, or "onset speed" of hunting, of a vehicle is defined as the lowest speed at which one of the lateral or yaw vibration modes becomes the least-damped mode, resulting in self-sustained oscillations of more pronounced amplitudes.

The rms, absolute peak and peak L95 levels of the lateral accelerations were computed for all vehicle speeds in the frequency range of Ø to 2Ø Hertz. Hunting was said to start at that particular speed where a sharp increase in the acceleration levels was observed. The state of the motion in which full flange-to-flange hunting occurred was determined by examining the respective wheel/rail profile geometrical data obtained from field measurements, as well as from the typical limit cycle behavior, which manifests itself in a steady-state-like motion, seen on the acceleration time histories.

In general, the lateral dynamics of a freight car involve the coupled sway and yaw oscillations of the car body, as well as lower and upper car body motions. Hence, the lateral accelerations recorded at the center of gravity of the leading and trailing ends of the vehicle, were combined to give car body yaw and sway accelerations, which were then used to determine the dominant modes of car body hunting.

4.1 Hunting with CN Heumann (Radford) Wheel Profiles

The empty car, equipped with CN Heumann (Radford) wheel profiles, experienced sporadic hunting at 51 mph. It was seen

from the acceleration time history plots that hunting first occurred at the leading end of the vehicle, where both the car body and the truck moved together as a rigid body with large amplitude oscillations. It should be mentioned that the hunting motion of the leading end of the vehicle with respect to the trailing end has been referred to as a "nosing" motion. During this "nosing" motion, the two trucks and the car body experience different amplitudes of lateral oscillations, with the leading end having larger amplitudes and higher frequencies.

The rms lateral accelerations calculated at different speeds for the car body and axles are shown in Figures 13 and 14, where the sharp increase in the rms accelerations at 51 mph indicated the onset of hunting for the leading end of the vehicle. In this configuration, the stability of the vehicle at both the car body CG and axles was characterized by the rms accelerations which exceeded the Ø.1 g level; this is the level above which hunting took place, but below which it did not. The sporadic hunting of the trailing end of the vehicle started at 56 mph, at which point the rms accelerations also exceeded the Ø.1 g level. The intermittent hunting of the leading end continued with increasing speeds and larger amplitudes of lateral accelerations. Fully sustained hunting of the leading end was evidenced at speeds above 56 mph. During sustained hunting of the leading end, however, the trailing end was still undergoing sporadic hunting with more pronounced oscillation amplitudes.

The leading and trailing end car body accelerations converted into yaw and lateral accelerations indicated that the car body

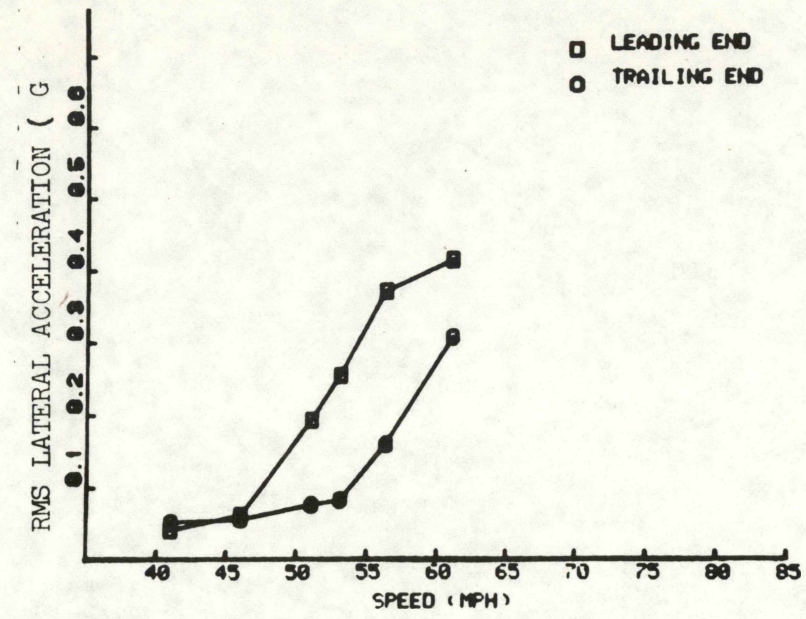

Figure 13. Root-mean-square Lateral Acceleration at the Empty Car Body Center of Gravity vs. Speed, for CN Heumann (Radford) Wheel Profiles.

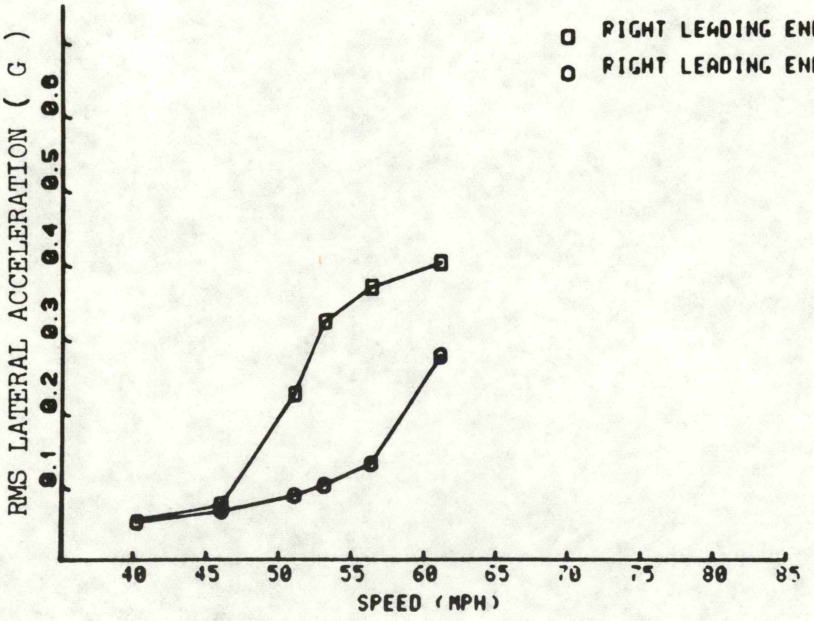

Figure 14. Root-mean-square Lateral Axle Acceleration vs. Speed, for CN Heumann (Radford) Wheel Profiles.

hunting essentially took the form of coupled yaw and sway oscillations.

A power spectral density analysis was performed to determine the frequencies associated with the various modes of hunting. The acceleration autospectra computed for the car body and axles revealed several dominant peaks, some of which were believed to have represented either peaks in the excitation spectrum or normal vehicle modes in the lateral plane. The most prominent peak center frequency, corresponding to the damped natural frequency of the least damped mode, represented the energy of the oscillations associated with hunting. The frequency of the lateral oscillations increased with increasing amplitudes of the motion; the frequencies computed at the various stages of hunting ranged from 3.25 Hertz at the start of intermittent hunting to 3.6 Hertz during fully sustained hunting. In Figure 15, the prominent car body frequencies are shown as a function of vehicle speed, where the frequency of the motion increased with speed, as the amplitudes of motion and subsequently the effective wheel conicity, increased. An important observation regarding the lateral stability of the vehicle was that, as full flange hunting whose motion was restricted by the wheel flanges took place, the amplitudes and frequency of the motion remained constant, a typical limit cycle behavior seen in nonlinear systems.

Another significant feature seen in most of the autospectra was that the narrow band high frequency peaks near 7.0 and 10.5 Hertz were observed to occur with considerable power. A thorough examination of the various autospectra indicated that, during any

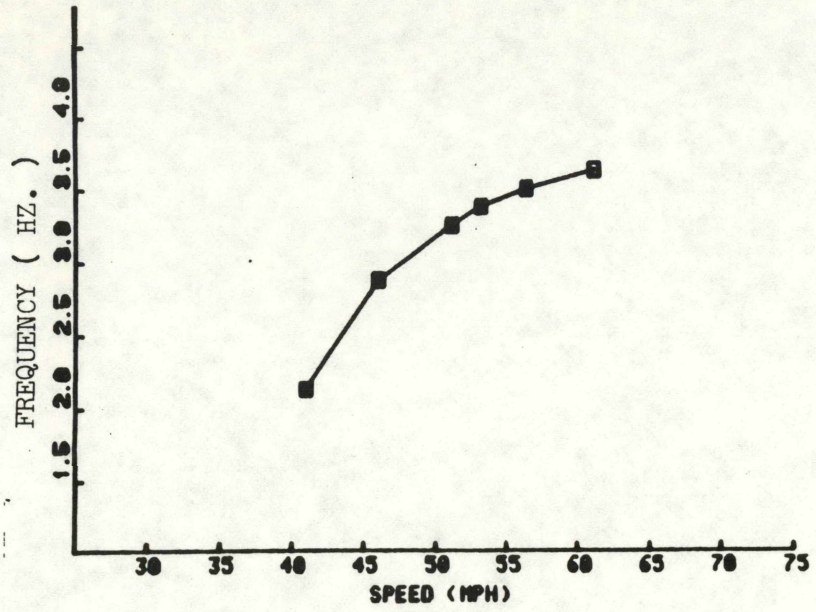

Figure 15. Empty Car Body Lateral Frequency vs. Speed, for CN Heuman (Radford) Wheel Profiles.

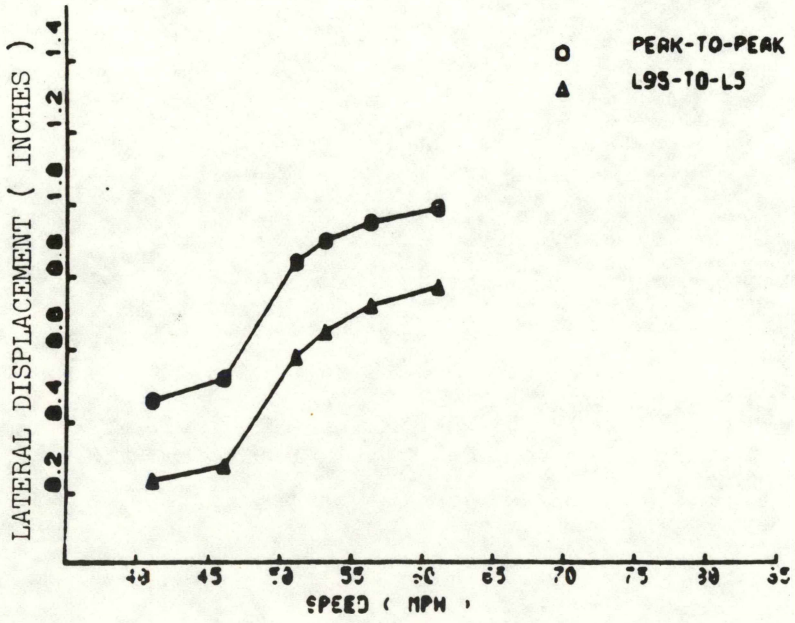

Figure 16. Leading Wheelset Lateral Displacement vs. Speed, for CN Heumann (Radford) Wheel Profiles.

stage of hunting motion, the dominant hunting frequencies were accompanied by high frequency components which were multiples of this critical frequency, i.e., superharmonic vibrations. With the very small amount of damping available during sustained hunting, it is possible that the energy from the first harmonic was transferred to its higher harmonics.

The wheel/rail displacements were measured and the resulting data processed to give lateral wheelset displacements at the wheel/rail interface. Figure 16 shows the peak-to-peak levels of these displacements, as a function of speed. The peak-to-peak wheelset excursions associated with the onset of hunting are believed to have taken place in the tread region of the wheel. However, wheelset excursions greater than Ø.5 inch may have resulted in flange contact. During sustained hunting, the peak-to-peak displacements of up to 1.Ø inch were indicative of full flange-to-flange hunting.

The lateral loads developed on the leading wheelset of the leading truck were also investigated. Of primary concern was the determination of the typical lateral loads produced at the onset of hunting, as well as during fully sustained hunting. It was found that peak lateral loads of up to 13,5ØØ lbs were developed during sustained hunting. Figure 17 shows the leading axle lateral loads as a function of speed. It was also found that the lateral loads, with a track distance duration of 6 feet, exceeded the maximum lateral loads recommended in the performance guidelines.

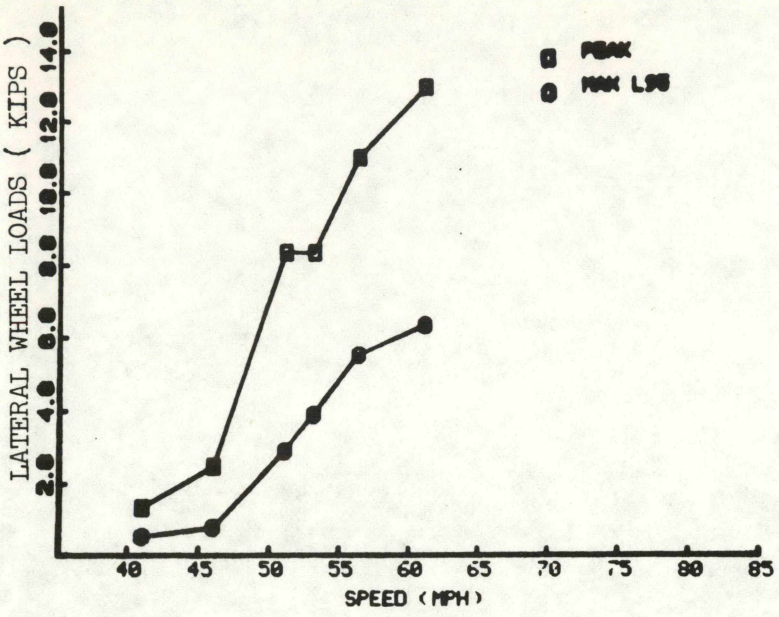

Figure 17a. Lateral Load vs. Speed, for the Right Wheel of the Leading Axle, CN Heumann (Radford) Wheel Profiles.

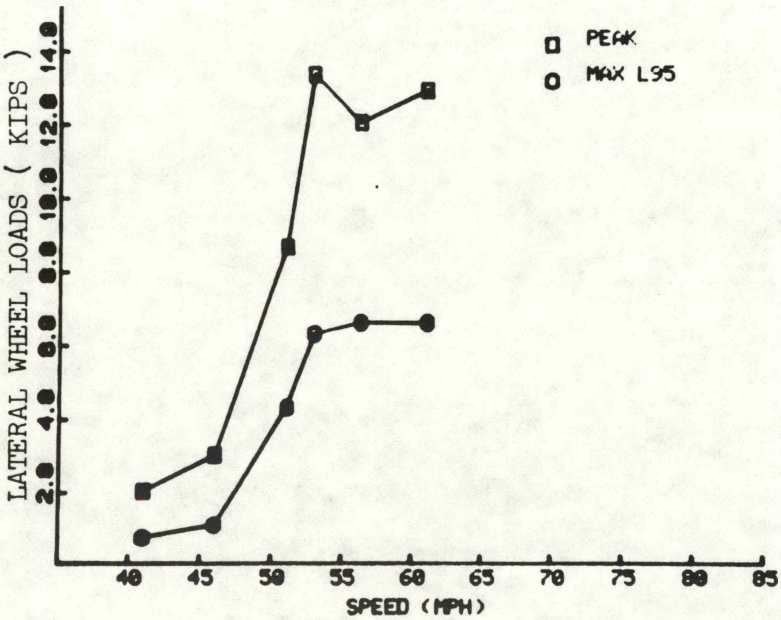

Figure 17b. Lateral Load vs. Speed, for the Left Wheel of the Leading Axle, CN Heumann (Radford) Profiles.

4.2 Hunting with 0.3 Conicity Wheel Profiles

It was found that the vehicle with 0.3 conicity wheel profiles experienced sporadic hunting at 45 mph, which is lower than that with a CN Heumann (Radford) profile. This is obviously due to the destabilizing effect of the higher conicity on the lateral dynamics of the vehicle.

At the onset speed of hunting, the leading end of the vehicle at both the car body and axles exhibited sporadic hunting behavior and the two systems moved as a rigid body. Although the leading end went into sporadic hunting, the trailing end axle and car body did not display any instability.

Figures 18 and 19 show the rms lateral accelerations for both the car body and axles, respectively, as a function of speed. Although the response of the vehicle was stable at speeds up to 40 mph, the rms accelerations exceeding 0.1 g at 45 mph were indicative of the onset of hunting. Unlike the vehicle with CN Heumann (Radford) wheel profiles, the amplitudes of the oscillations on the trailing end increased rather rapidly. The sharp increase in rms accelerations between 45 and 50 mph indicated the initiation of intermittent hunting for the trailing end, where the rms accelerations were also above the 0.1 g level. At increasing speeds, the amplitudes of the lateral oscillations rapidly increased at both the leading and trailing ends of the vehicle undergoing sporadic hunting. At the highest test speed of 55.5 mph, sustained oscillations were developed, in which the rms accelerations exceeded the 0.3 g level. At the trailing end, the oscillations of motion were somewhat sustained, that is, the

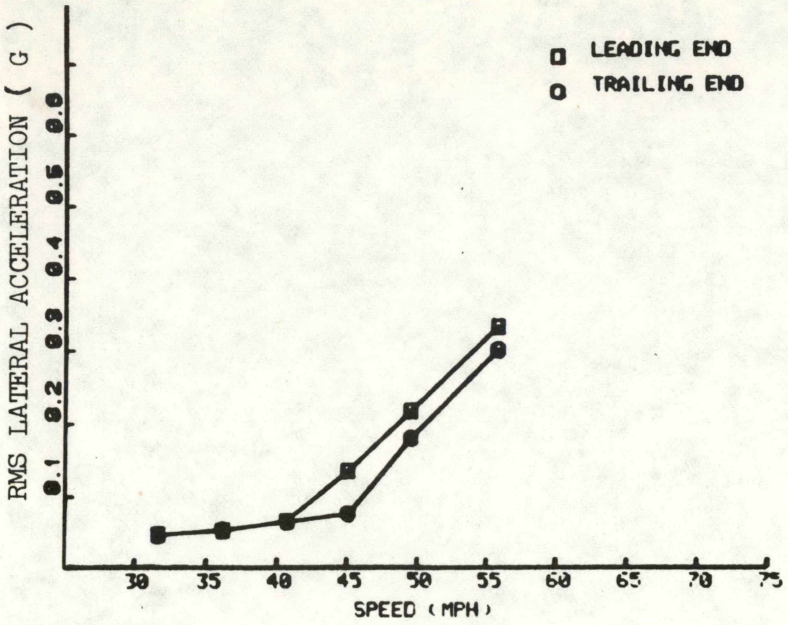

Figure 18. Root-mean-square Lateral Acceleration at the Empty Car Body Center of Gravity vs. Speed, for Ø.3 Conicity Wheel Profiles.

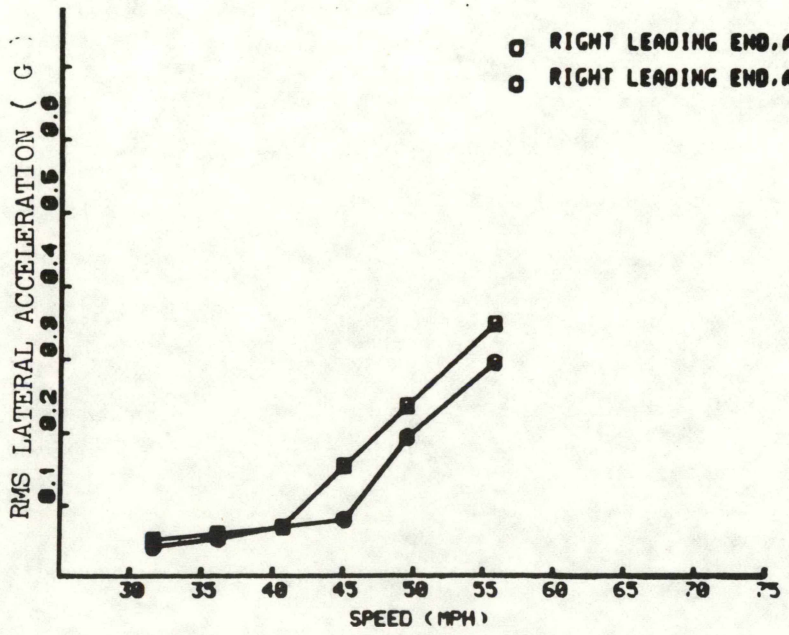

Figure 19. Root-mean-square Lateral Axle Acceleration vs. Speed, for Ø.3 Conicity Wheel Profiles.

amplitudes of the oscillations were still variable with position along the track.

At speeds near 60 mph, it is believed that the car body and axles would probably undergo fully sustained hunting with very large oscillations. Safety requirements prevented the car from being tested at these higher speeds.

One of the most important phenomenon, which occurred with 0.3 conicity wheels, was the car body yaw and sway accelerations computed by combining the leading and trailing end car body lateral accelerations [3]. In the case of sustained hunting, it was found that the car body experienced almost uncoupled motions, in which the energy was transferred from one mode to another. When the car body yaw motion dominated, the amplitudes of the sway acceleration were considerably attenuated, and vice versa. It should be mentioned here that, in the case with CN Heumann (Radford) wheel profiles car, body hunting had been found to consist of mostly coupled lateral and yaw oscillations.

The hunting oscillation frequencies were similar; at the onset of hunting the frequency was 3 Hertz and during sustained hunting it was 3.5 Hertz. The high frequency peaks which appeared in the acceleration autospectra near 7 and 10.5 Hertz were attributed to the second and third harmonics of the hunting frequency, as the nonlinearities in the system provided a mechanism by which energy could be transferred to the higher harmonics.

On the basis of the test data analysis, it was concluded that the onset of car body hunting could be characterized by rms

accelerations exceeding Ø.1 g. The quantified levels of car body lateral accelerations during sustained hunting were Ø.3 g rms, with the axle accelerations being slightly higher. Full flange hunting of the vehicle could only be conjectured, since the wheelset displacements were not measured for this profile configuration. A comparison of the acceleration levels with Ø.3 conicity and CN Heumann (Radford) wheel profiles, however, revealed that the vehicle with Ø.3 conicity wheels must have experienced full flange hunting at its leading end. Sustained hunting was also evident during on-site test observations.

4.3 Hunting with AAR 1:2Ø Wheel Profiles

For the hunting tests with AAR 1:2Ø wheel profiles, the results differed somewhat. Throughout the range of test speeds, up to 75 mph, the response of the vehicle was stable. The lateral oscillations of the vehicle were mainly due to random track irregularities and the rms lateral accelerations remained below the Ø.1 g level. At 81 mph, however, high amplitude intermittent hunting started simultaneously at both the leading and trailing ends of the vehicle. Peak rms accelerations of Ø.43 g for the A-end car body, and Ø.45 g for the AR4 axle indicated that the vehicle hunting was probably accompanied by full flange oscillations, which was also observed by the test crew. The amplitudes of the oscillations at the trailing end were on the same order of magnitude. Figures 2Ø and 21 show the rms car body and axle accelerations as a function of speed for this configuration.

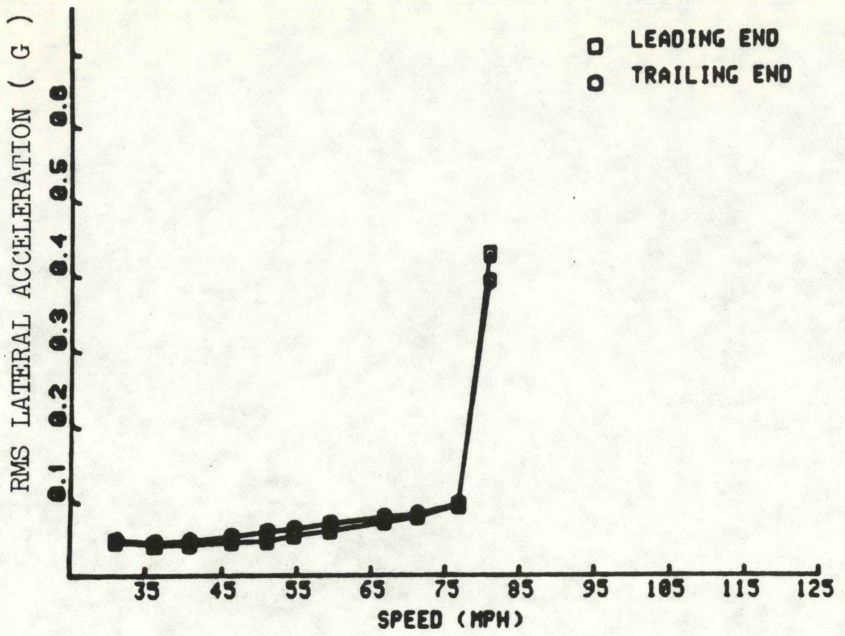

Figure 20. Root-mean-square Lateral Acceleration at the Empty Car Body Center of Gravity vs. Speed, for AAR 1:20 Wheel Profiles.

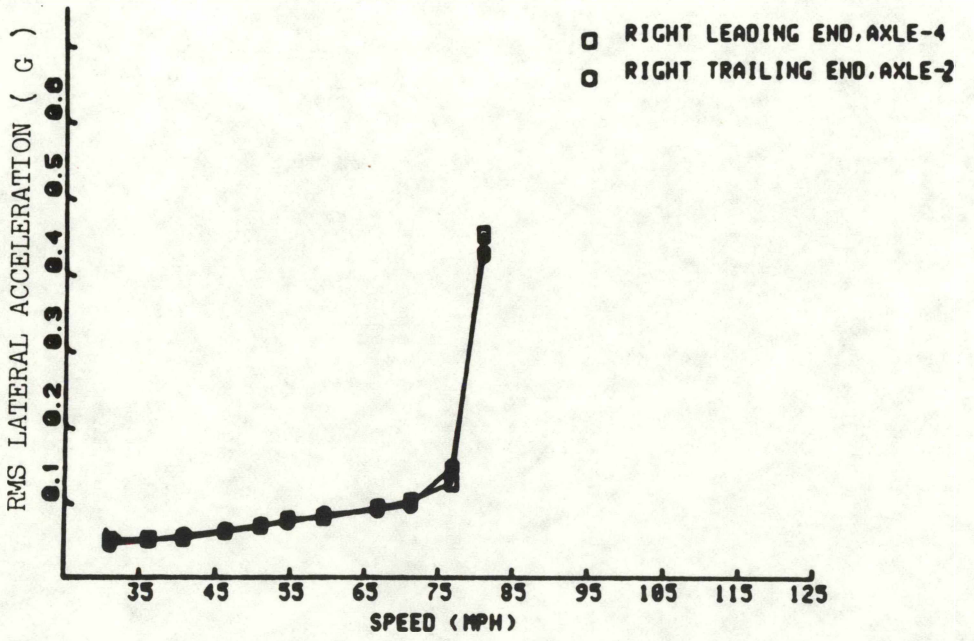

Figure 21. Root-mean-square Lateral Axle Acceleration vs. Speed, for AAR 1:20 Wheel Profiles.

The autospectra computed for the car body and axles revealed peaks at similar frequencies. The major peak at 3.5 Hertz was accompanied by another at 3.38 Hertz, indicating a coupled body and truck hunting. The higher frequency components of the motion were similar to those with the other wheel profiles. Two peaks near 7.Ø and 1Ø.5 Hertz, both with substantial power, were noted.

4.4 Effect of Wheel Conicity on Hunting

An estimation of the wheel conicity which corresponds to the actual running condition at the onset of hunting is a difficult task. This is due, in part, to wheelset equilibrium changes, which are strongly affected by rail profile variations. Evaluation of the wheel-rail geometry constraint functions in the linear conicity region indicated that the effective conicity varied from Ø.1 for CN Heumann (Radford) profiles to Ø.2 for the Ø.3 conicity wheel profile. The wheel profiles were not measured for the case with AAR 1:2Ø wheels, however it was assumed that the corresponding conicity was approximately Ø.Ø5. The results of wheelset displacement measurements with CN Heumann (Radford) profiles showed that, at the onset of hunting, the peak wheelset excursions caused occasional flange contact, resulting in higher effective conicities. Therefore, the effective conicities given above pertained to stable motions. The vehicle equipped with CN Heumann (Radford) profile wheels hunted at 51 mph, as opposed to 45 mph for the case of Ø.3 conicity wheels. It is therefore evident that, at the onset of hunting, higher effective conicities prevailed for the case with Ø.3 conicity wheels. Hence, it can be

concluded that the critical speed of the vehicle increased as the wheel conicity decreased.

It should also be noted that once fully sustained hunting occurred, the amplitudes of the motion reached a level that was restricted by the wheel flanges.

For all three wheel profiles, similar acceleration levels during comparable hunting conditions have been found. The most stable case was with an AAR 1:20 wheel profile, which experienced lateral instability at speeds near 81 mph. However, low conicity conflicts with the requirements for better curving performance. Hence, vehicle designs that foster better dynamic performance require not only the implementation of alternative wheel profiles, but better truck and suspension system designs. The purpose of this test program was to encourage such new designs.

Table 1 summarizes the acceleration levels at the "onset" of hunting, and at the "sustained" hunting speeds.

5.0 CURVING REGIME

The primary objective of the data analysis in the curving regime was to determine the performance of the loaded car during steady state curve negotiation, as well as to evaluate its dynamic response when entering into and exiting from these curves. Performance of the vehicle was characterized by using wheel/rail forces, L/V ratios, and angles-of-attack. The following is a summary of the results obtained. A detailed analysis can be found in [4].

Table 1. Summary of Acceleration Measurements for the Hunting Regime

Wheel Profile

Accelerometer Locations	CN Heumann (Radford)				0.3 Conicity				AAR Standard 1:20	
	Root-mean-square Levels		Peak Levels		Root-mean-square Levels		Peak Levels		Root-mean-square Levels	Peak Levels
	51mph	61mph	51mph	61mph	45mph	56mph	45mph	56mph	81mph	81mph
Carbody										
At C of G "A" End	0.19	0.42	0.56	1.10	0.14	0.35	0.37	0.84	0.43	1.30
At C of G "B" End	0.15	0.30	0.36	0.90	0.18	0.30	0.47	0.73	0.43	1.30
Bearing Adapter										
At AR4	0.16	0.45	0.95	1.51	0.16	0.35	0.59	1.04	0.45	1.50
At BR2	0.13	0.28	0.80	1.00	0.19	0.30	0.63	0.88	0.43	1.40

5.1 Wheel/Rail Forces

The forces developed between the wheel and rail depend upon the wheel/rail geometry, such as wheel profiles, degree of track curvature, superelevation and direction of train travel, as well as creep forces and creep moments, which result from elastic deformations of the wheel and rail in the contact region.

On sharp curves, depending upon the speed of the vehicle, the outer wheel of the leading and/or trailing axle may assume flange contact with the high rail. This situation contributes to the wear of the wheel flanges, as well as the gage face of the high rail.

Figures 22 and 23 present the results of the leading axle lateral wheel loads on the 5 degree curve, as a function of test speed, for the CW and CCW runs, respectively. It should be noted that, in order to avoid overlapping of the curves, the signs of the low rail lateral wheel loads were changed; thus the negative sign is indicative of a low rail lateral load directed towards the wheel flange. As seen in these figures, the lateral loads shifted to the high rail with increasing speeds, and the individual reaction forces on the rail acted to spread the rails apart, which could result in gage widening of the track.

The mean values of the lateral loads, computed near balance speed as a function of track curvature, are shown in Figures 24 and 25, for the CW and CCW runs, respectively. A close examination of these figures reveals that the lateral loads showed differences depending upon the direction of train travel. For almost all of the curving tests, it was found that the high rail

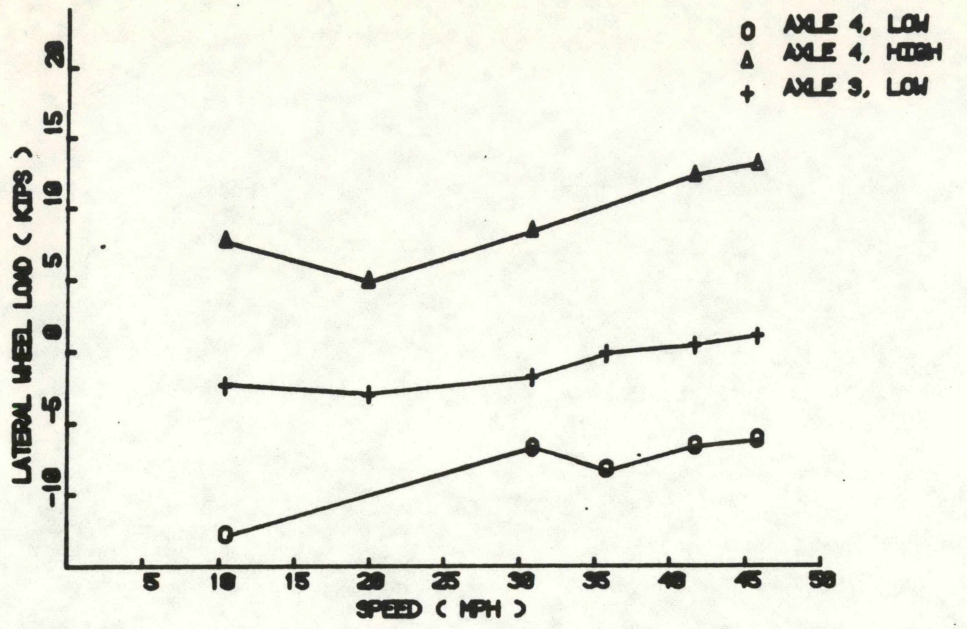

Figure 22. Lateral Wheel Load vs. Speed, for a 5 Degree Curve in the Clockwise Direction.

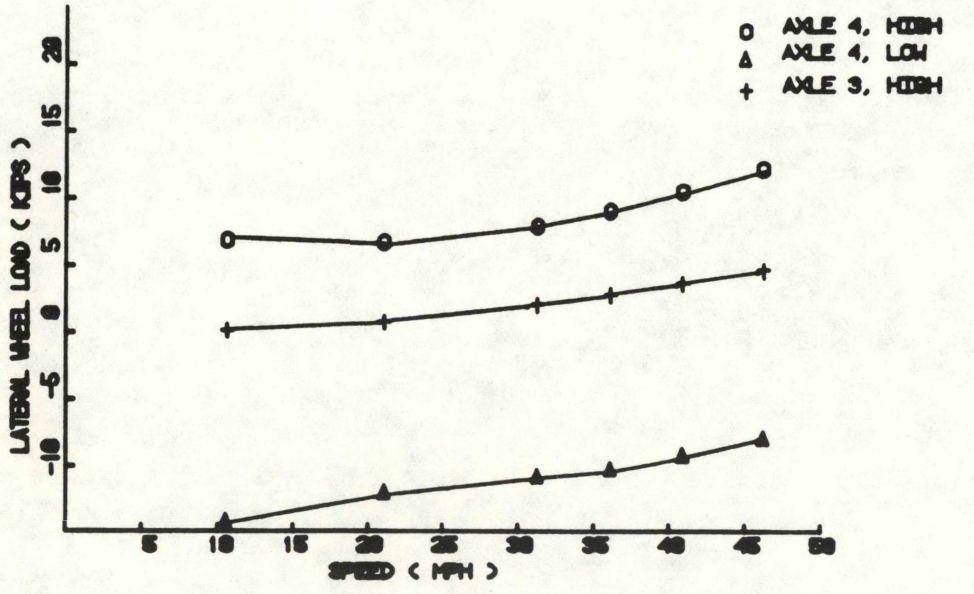

Figure 23. Lateral Wheel Load vs. Speed, for a 5 Degree Curve in the Counterclockwise Direction.

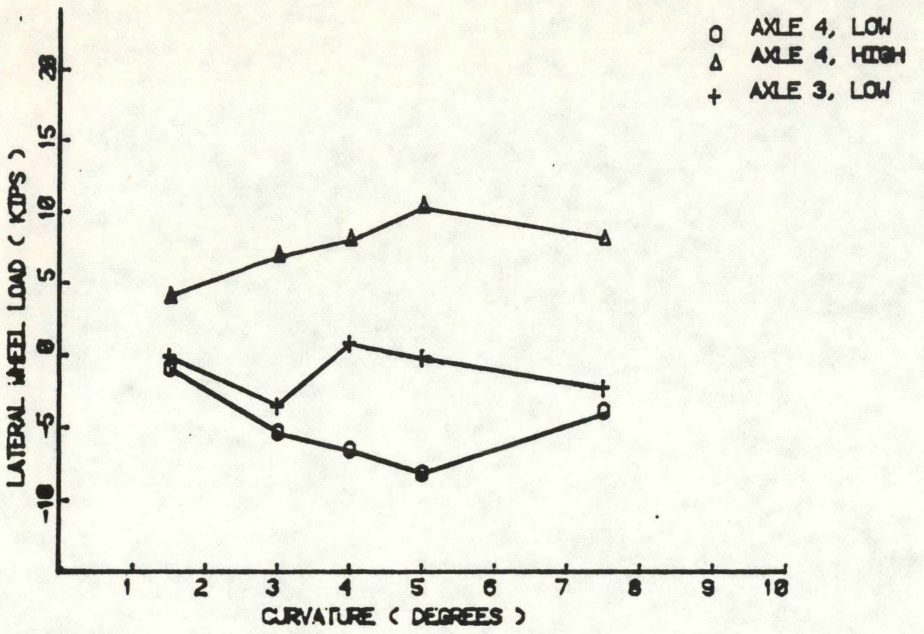

Figure 24. Lateral Wheel Load vs. Track Curvature, at Balance Speed in the Clockwise Direction.

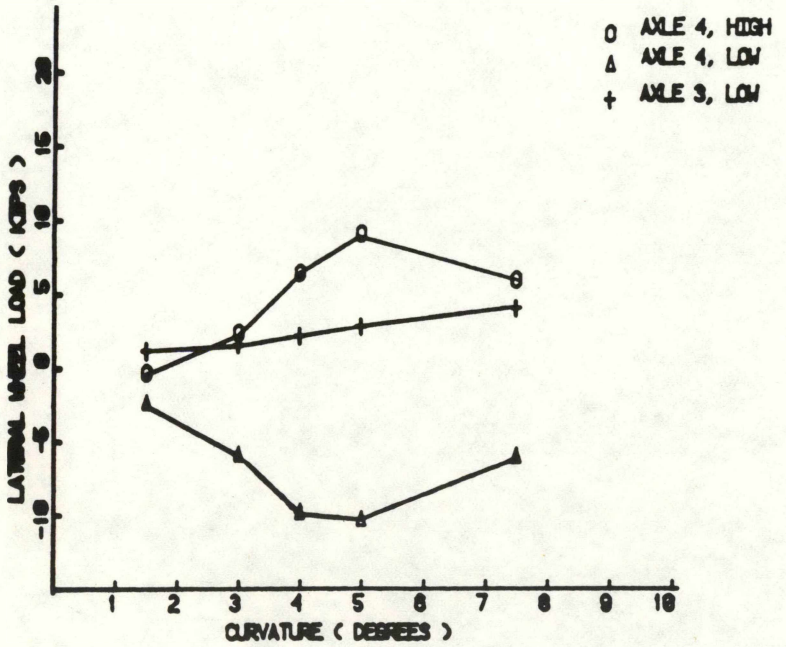

Figure 25. Lateral Wheel Load vs. Track Curvature, at Balance Speed in the Counterclockwise Direction.

lateral and vertical loads in the CW direction were higher than those in the CCW direction, and the low rail wheel loads in the CCW direction were higher than those in the CW direction. It was concluded from the vertical load data that an asymmetric load distribution, resulting in higher loading of the left side of the truck, was present and resulted in a directional preference during curving. However, "truck memory," as the vehicle moved from one curve to another, an asymmetric suspension system and different curve entry conditions may also have contributed to this phenomenon.

In order to evaluate the maximum levels of lateral loads which could cause permanent track deformation, the net axle loads, over a 6-foot distance duration, were investigated at severe unbalance conditions on the 5 degree curved test track. It was found that the maximum net lateral leading axle load at 45 mph, corresponding to a 3-inch unbalanced superelevation, was as high as 15,700 lbs, directed towards the outside of the curve. At 10 mph, representing a 3.6-inch excess superelevation, the maximum axle load was on the order of 13,200 lbs, directed towards the inside of the curve. According to the performance criterion regarding permanent track deformation, the limiting level of axle load was recommended to be 20,500 lbs for the loaded car. It should be noted that the TTC tracks, where the tests were conducted, are maintained in good condition, e.g., FRA Class 4 or 5.

The L/V ratio has been widely used as a derailment index in evaluating the curving performance of railroad vehicles. In the

performance guidelines, the allowable limits of L/V ratios were established with regards to derailment safety of the prototype cars. Therefore, in this analysis, the performance criterion regarding wheel climb derailment was addressed in sharp curving situations. The maximum values of L/V ratios that were continuously sustained over 6 feet of track, LTD6MAX, were used to study their time durations.

The performance guidelines recommended a limiting L/V of Ø.8, with time durations corresponding to 6 feet of track for prototype cars with improved performance. This safety limit was to be used as a measure of the derailment propensity of covered hopper cars by wheel climb. The maximum levels of L/V ratios, with 6 feet distance durations, were computed for the 3.Ø, 4.Ø and 5.Ø-degree curves at 45 mph and for the 7.5-degree curve at 4Ø mph, as shown in Figures 26 and 27. Maximum L/V ratios of up to Ø.6 were experienced on the 5-degree curve in the CCW direction. Examination of the corresponding L/V ratio and wheelset yaw angle time histories revealed that higher amplitudes of L/V ratios were accompanied by higher wheelset angles-of-attack, with longer time durations.

Based on the data presented above, the performance of the vehicle with respect to high L/V ratios, that might cause a wheel climb derailment, complied with the performance criterion. However, in revenue service, derailments by wheel climb can also occur from the additional effects of high amplitude track perturbations that are present in the track under comparable curving situations.

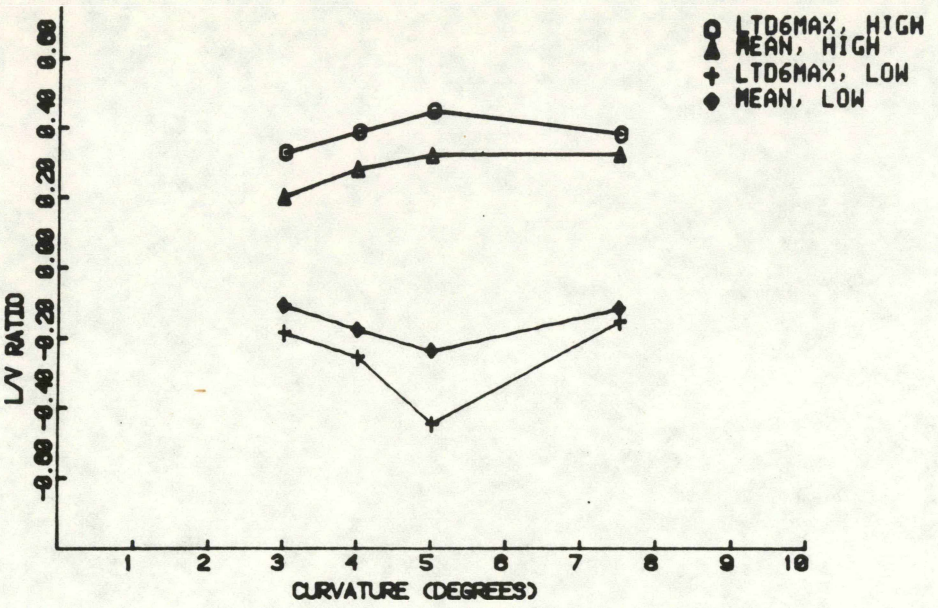

Figure 26. L/V Ratio vs. Track Curvature, for a Speed of 45 mph in the Clockwise Direction.

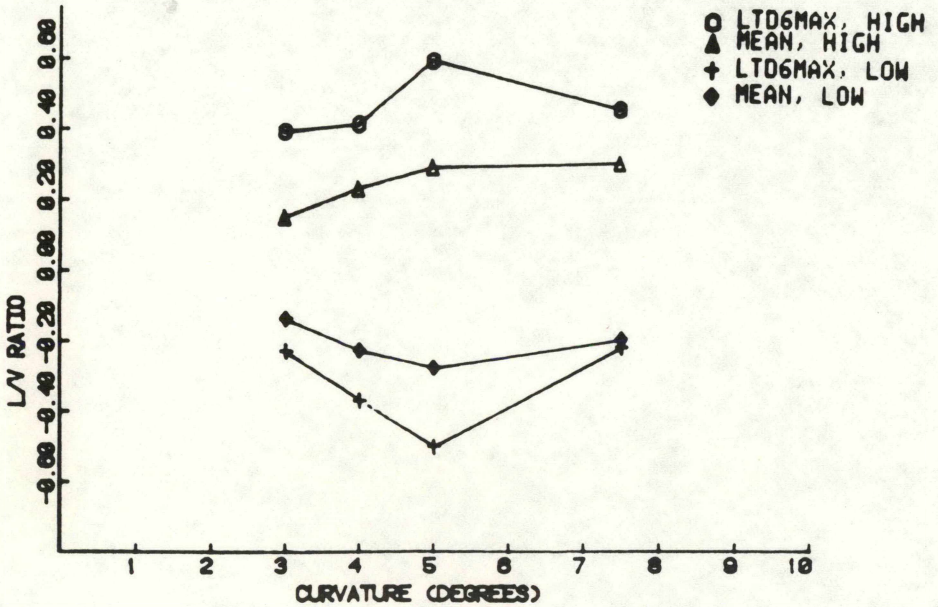

Figure 27. L/V Ratio vs. Track Curvature, for a Speed of 45 mph in the Counterclockwise Direction.

5.2 Wheelset Angle-of-attack

The angles-of-attack of a wheelset were computed from the wheel/rail displacement measurements. Because of difficulties in obtaining an absolute datum for the wheel/rail probes, it was impossible to obtain an absolute value of angle-of-attack on tangent track sections. Hence, the angles-of-attack in curves were computed as the increments from tangent to curve. The results of the analysis indicated a general conformity, in that the greater angles-of-attack were found to be associated with the higher track curvatures. In general, the leading wheelset experienced higher values of angle-of-attack, yawing behind the radial line extending from the center of the curve through the center of the wheelset axle. The trailing wheelset, however, consistently experienced yaw angles that were near zero, thus remaining in its radial position. Figures 28 and 29 show the angles-of-attack, computed near balance speed, as a function of track curvature, for the CW and CCW runs, respectively.

6.Ø SPIRAL TWIST REGIME

Due partly to its body stiffness in twist, the base car has been known to experience difficulties in entering and exiting sharper curves of relatively short spiral lengths. As a part of the dynamic performance tests, the vertical dynamics of the empty car in curve entry has been addressed in the "bunched spiral" tests. The existing spiral into a 7.5-degree curve in the Balloon loop was modified to configure a bunched spiral section with severe twist. The existing spiral was modified to have no

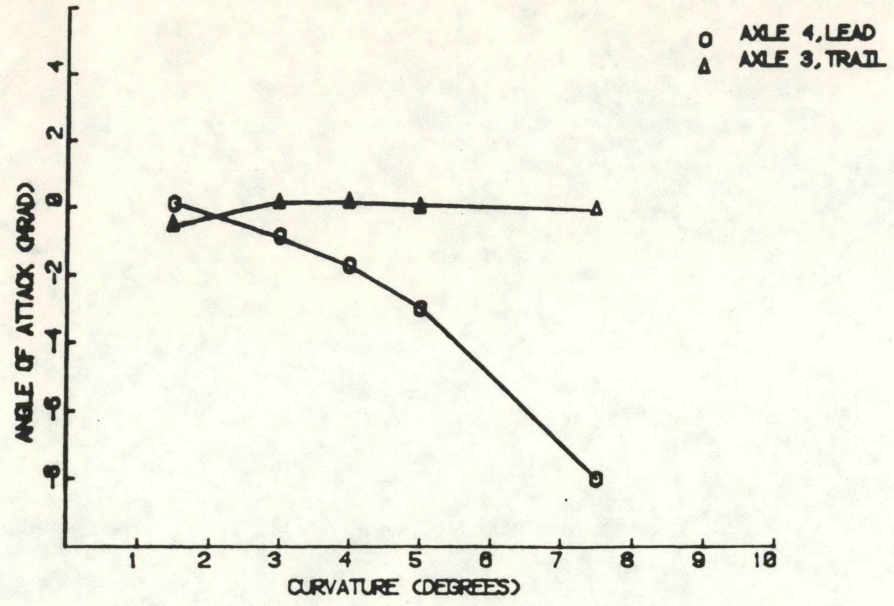

Figure 28. Angle-of-attack vs. Track Curvature, for the Clockwise Direction.

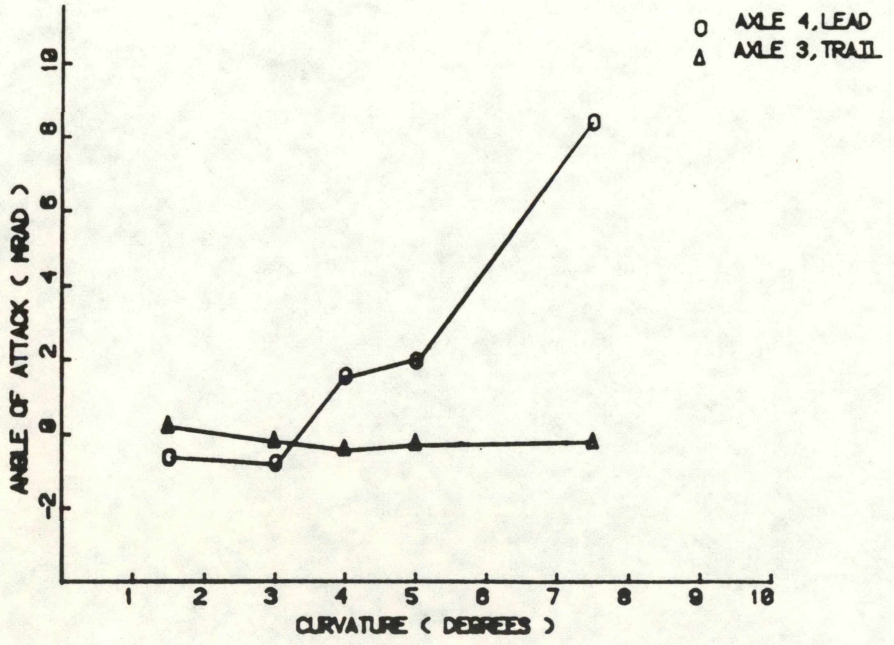

Figure 29. Angle-of-attack vs. Track Curvature, for the Counterclockwise Direction.

superelevation for the first 120 feet. Over the next 120 feet, the superelevation was made to increase from zero to 4.5 inches and remained constant thereafter. This track configuration is shown in Figure 30.

Results of the data analysis pertaining to the empty car spiral twist tests provided valuable information regarding the derailment tendency by vehicle overturning. Wheel unloadings as high as 80 percent, with almost 100 milliseconds of time duration, were developed on the low rail by the leading axle wheelset at 40 mph. Figures 31 and 32 show how the leading axle vertical loads changed as a function of speed. When environmental effects, such as wind loading and track perturbations, along with the inertial forces produced by the higher lateral accelerations are included, they may unavoidably contribute to the tendencies of the vehicle to derail. At most test speeds, the vertical wheel forces exhibited severe load fluctuations, caused partly by the wheel flanges repeatedly contacting the rails and partly by the effects of the high body twist, resulting in a severe weight shift. The resulting vertical loads were high enough to create dynamic load factors more than twice the static load. The time durations associated with these loads were, however, relatively short. The maximum wheel loads that were continuously sustained over 6 feet of track were on the order of 11,000 lb.

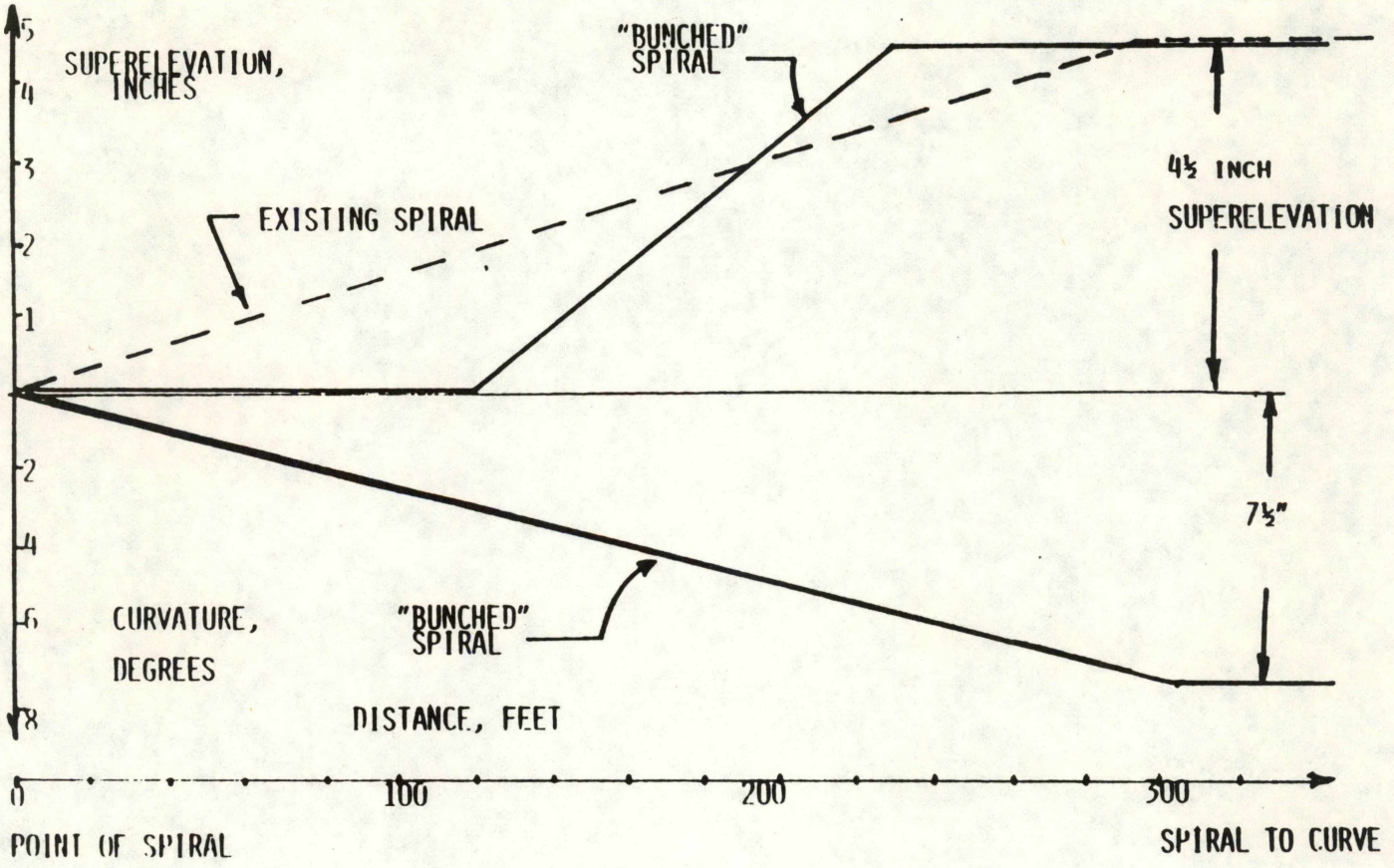

Figure 30. Spiral Twist Curve Configuration.

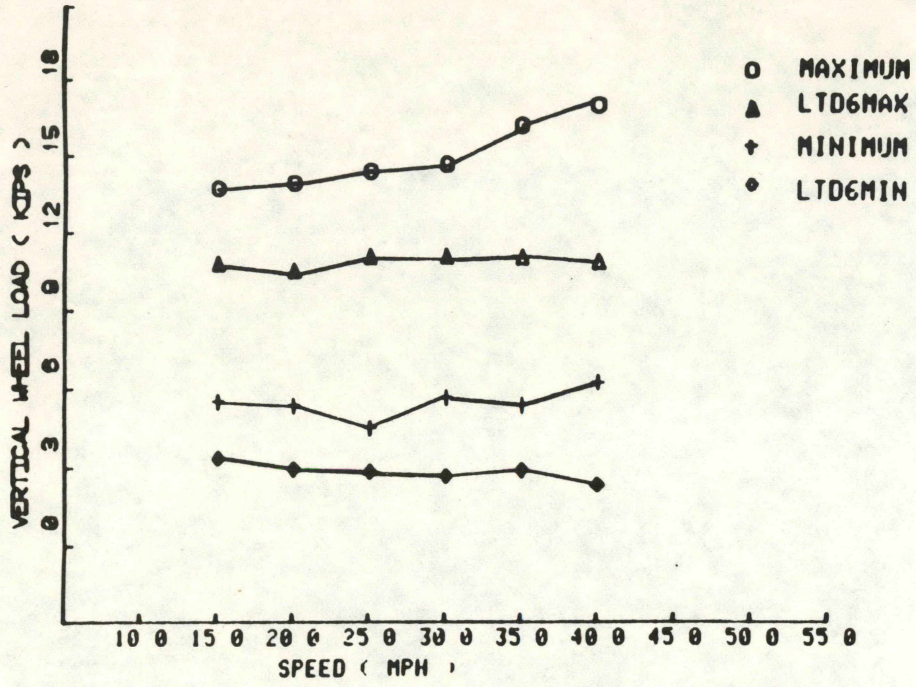

Figure 31. Leading Axle Low Rail Wheel Vertical Load vs. Speed, for the Spiral Twist Regime.

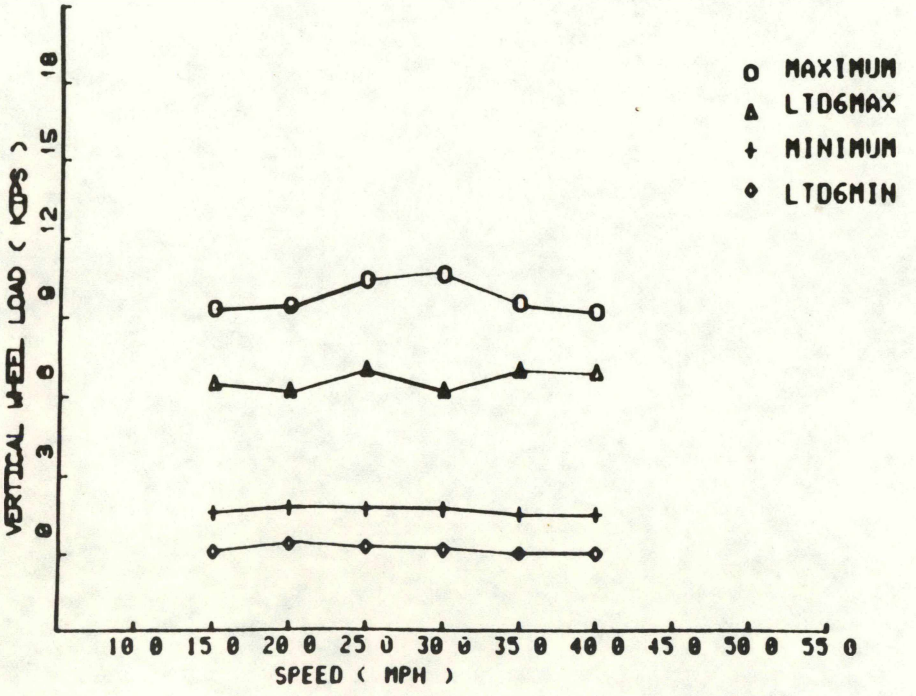

Figure 32. Leading Axle High Rail Wheel Vertical Load vs. Speed, for the Spiral Twist Regime.

7.Ø REFERENCES

1. Manos, W.D, and Johnstone, B., "Performance Guidelines - High Performance/High Cube Covered Hopper Car," Association of American Railroads, Report No. R-423, Chicago, Illinois, June, 198Ø.

2. Kalaycioglu, S.F., and Punwani, S.K., "High Performance High Cube Covered Hopper Program, Base Car Dynamic Performance Tests, Volume 1 - Rock and Roll and Bounce," Association of American Railroads, Report No. R-566, Chicago, Illinois, April, 1984.

3. Kalaycioglu, S.F., and Punwani, S.K., "High Performance High Cube Covered Hopper Program, Base Car Dynamic Performance Tests, Volume 2 - Hunting," Association of American Railroads, Report No. R-568, Chicago, Illinois, April, 1984.

4. Kalaycioglu, S.F., and Punwani, S.K., "High Performance High Cube Covered Hopper Program, Base Car Dynamic Performance Tests, Volume 3 - Curving," Association of American Railroads, Report No. R-572, Chicago, Illinois, April, 1984.

5. Punwani, S.K., Johnson, M.R., Joyce, R.P., and Mancillas, C., "Measurement of Wheel/Rail Forces on the High Cube, High Performance Covered Hopper Car Project," Proceedings of the ASME Rail Transportation Spring Conference, Chicago, Illinois, 1984.

6. Bendat, J. S., and Piersol, A. G., Random Data: Analysis and Measurement Procedures, Wiley - Interscience, 1971.

8.Ø APPENDIX A

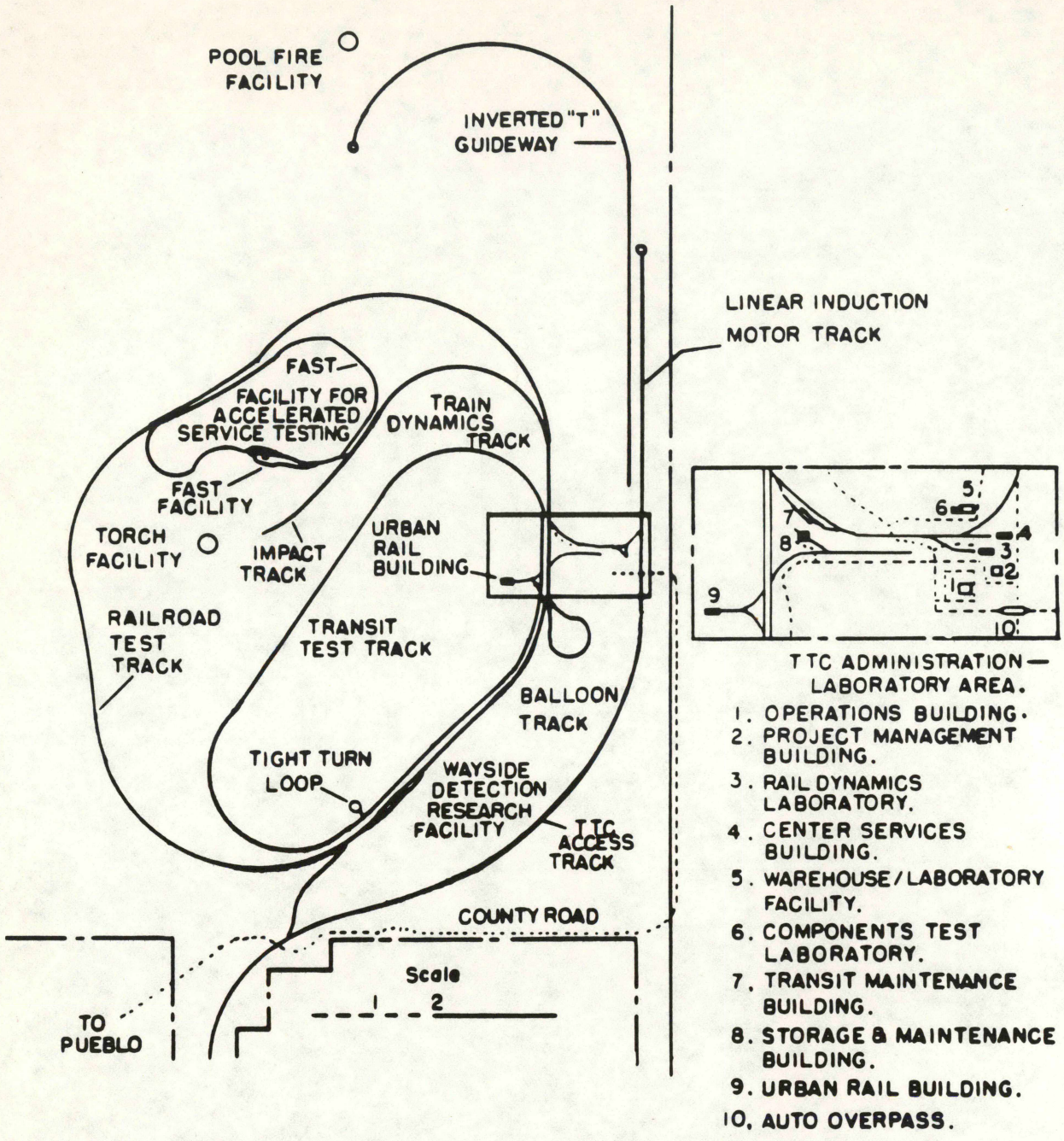

Figure A-1. Schematic Diagram of the Transportation Test Center at Pueblo, Colorado, Showing Various Test Track Locations.

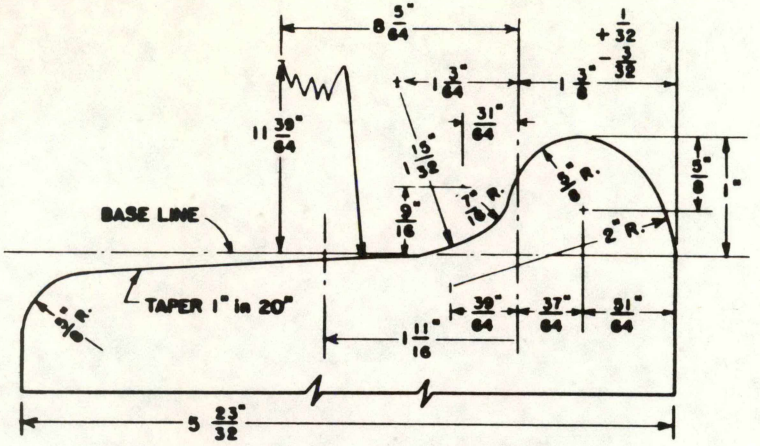

CN Heumann (Radford) Profile

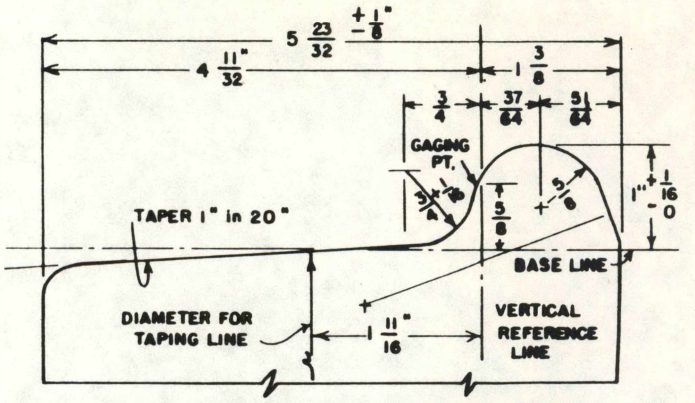

AAR Standard 1:20 Profile

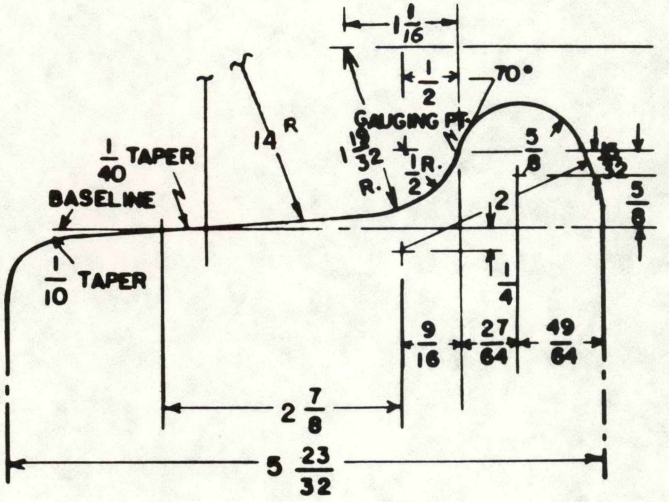

Ø.3 Conicity Profile

Figure A-2. Wheel Profiles Used in the Hunting Tests.

High Performance, High Cube Covered Hopper Program Base Car Dynamic Performance Tests: Volume 4- Summary (TTD), 1984 -Association of American Railroads, SF Kalaycioglu, SK Punwani